A subjective Bayesian framework for synthesizing deep uncertainties in climate risk management

James Doss-Gollin[1,1,1] and Klaus Keller[2,2,2]

[1]Department of Civil and Environmental Engineering, Rice University
[2]Thayer School of Engineering, Dartmouth College

November 30, 2022

Abstract

Projections of nonstationary climate risks can vary considerably from one source to another, posing considerable communication and decision-analytical challenges. One such challenge is how to present trade-offs under deep uncertainty in a salient and interpretable manner. Some common approaches include analyzing a small subset of projections or treating all considered projections as equally likely. These approaches can underestimate risks, hide deep uncertainties, and are mostly silent on which assumptions drive decision-relevant outcomes. Here we introduce and demonstrate a transparent Bayesian framework for synthesizing deep uncertainties to inform climate risk management. The first step of this workflow is to generate an ensemble of simulations representing possible futures and analyze them through standard exploratory modeling techniques. Next, a small set of probability distributions representing subjective beliefs about the likelihood of possible futures is used to weight the scenarios. Finally, these weights are used to compute and characterize trade-offs, conduct robustness checks, and reveal implicit assumptions. We demonstrate the framework through a didactic case study analyzing how high to elevate a house to manage coastal flood risks.

A subjective Bayesian framework for synthesizing deep uncertainties in climate risk management

James Doss-Gollin[1], **Klaus Keller**[2]

[1]Department of Civil and Environmental Engineering, Rice University
[2]Thayer School of Engineering, Dartmouth College

Key Points:

- We introduce a Bayesian framework to transparently synthesize and characterize deep uncertainties with the goal to support decision-making.
- We demonstrate the framework using a simple case study of how high to elevate a house to manage coastal flood risks.
- Estimates of performance or robustness under deep uncertainty necessarily involve subjective judgments.

Corresponding author: James Doss-Gollin, jdossgollin@rice.edu

Abstract

Projections of nonstationary climate risks can vary considerably from one source to another, posing considerable communication and decision-analytical challenges. One such challenge is how to present trade-offs under deep uncertainty in a salient and interpretable manner. Some common approaches include analyzing a small subset of projections or treating all considered projections as equally likely. These approaches can underestimate risks, hide deep uncertainties, and are mostly silent on which assumptions drive decision-relevant outcomes. Here we introduce and demonstrate a transparent Bayesian framework for synthesizing deep uncertainties to inform climate risk management. The first step of this workflow is to generate an ensemble of simulations representing possible futures and analyze them through standard exploratory modeling techniques. Next, a small set of probability distributions representing subjective beliefs about the likelihood of possible futures is used to weight the scenarios. Finally, these weights are used to compute and characterize trade-offs, conduct robustness checks, and reveal implicit assumptions. We demonstrate the framework through a didactic case study analyzing how high to elevate a house to manage coastal flood risks.

Plain Language Summary

Identifying sound strategies to manage risks driven by climatic changes is a complex task given the large uncertainties surrounding projections of coupled natural-human systems. These uncertainties often arise from choices experts have to make, for example about how to formulate scientific models of future water levels. Different experts can disagree about these choices, leading to different projections. Analyzing decisions in such a situation of deep uncertainty poses nontrivial challenges. For example, picking a single representative projection can under-estimate risk and result in poor decisions. Similarly, communicating results separately for each projection can overwhelm decision-makers. To make matters worse, typical approaches to this problem are mostly silent on what assumptions make a difference for the decisions at hand. We develop and demonstrate a framework to address these challenges. The framework provides a transparent approach to (i) combine a large number of deeply uncertain projections to a more interpretable sample set and (ii) provide insights about which assumptions and modeling choices influence decisions. We demonstrate the approach with a relatively simple example question of how high to elevate a house in the face of deeply uncertain projections of future water levels.

1 Introduction

Aging infrastructure and changes in regulations, finance, patterns of population and infrastructure use, and climate challenge the ability of critical infrastructures to meet design objectives (Doss-Gollin et al., 2021, 2020; Chester et al., 2020; Tye & Giovannettone, 2021; M. Ho et al., 2017). To achieve acceptable performance with reasonable planning efforts, current practice in engineering, infrastructure design, and regulation relies heavily on standards that specify design events or conditions that buildings and infrastructure should safely withstand (Bruneau et al., 2017). For example, the Federal Emergency Management Agency (FEMA), local governments, and engineering consultants produce local floodplain maps in many communities. Buildings in the designated floodplain are subject to specific regulations, such as flood insurance requirements as an eligibility requirement for federally backed mortgages (Kousky & Kunreuther, 2014) or minimum elevations for new construction (American Society of Civil Engineers, 2006; The Federal Emergency Management Agency, 2011). Although this paper focuses on flooding, similar approaches inform mitigation strategies for a wide range of other hazards (American Society of Civil Engineers, 2013).

Standards-based risk management frameworks have many advantages, including scalability, explainability, and simplicity. However, the choice of standard is a complex design and policy choice. Risk-based design and cost benefit analysis (Eijgenraam et al., 2014; van Dantzig, 1956; Xian et al., 2017) offer a quantitative framework for comparing possible standards by emphasizing "a proportionate response to risk, so that the amount invested in risk reduction is in proportion to the magnitude of the risk and the cost-effectiveness with which that risk may be reduced" (Merz et al., 2010). This provides a formal basis for choices such as protecting hospitals and critical infrastructure to a higher degree than ordinary buildings (American Society of Civil Engineers, 2013). However, these methods are silent on how standards should balance trade-offs, not only between cost and performance but also between other stakeholder values such as sense of place, distributive justice, and safety (Keller et al., 2021; Helgeson et al., 2022; Quinn et al., 2017; Bessette et al., 2017; Vezér et al., 2018).

Moreover, estimates of performance trade-offs require implicit or explicit assumptions about the likelihood of different possible futures. Current practice emphasizes nominally objective methods that can be applied consistently across locations. For example, the United States Geological Survey (USGS) Bulletin 17C specifies procedures for estimating flood frequency (England et al., 2019). Similarly, the National Oceanic and Atmospheric Administration (NOAA) Atlas 14 provides estimates of the intensity, duration, and frequency of extreme rainfall (Perica et al., 2018; National Weather Service & Office of Water Prediction, 2022). One statistical assumption these analyses make is stationarity (the assumption that past and future hazard come from the same probability density function (PDF)), but global climate change and local environmental changes have cast scrutiny on this assumption (Merz et al., 2014; Milly et al., 2008; Doss-Gollin et al., 2019). While some methods have been proposed for incorporating nonstationarity into risk analyses (see Salas et al., 2018, for a review), these assume specific forms of a trend which may not adequately represent physical processes or sample only a subset of uncertainties (Doss-Gollin et al., 2019; Montanari & Koutsoyiannis, 2014; Serinaldi & Kilsby, 2015). At least in part because of the challenges associated with developing objective methods to select from diverging projections of future hazard, official guidance continues to rely on the stationarity assumption (England et al., 2019; Perica et al., 2018).

The limitations of objectivist approaches to projecting risk extend beyond estimating nonstationary climate hazards. Human-natural systems are never closed and model results are never unique, and thus validation and verification of models representing these systems is necessarily qualitative and subjective (Oreskes et al., 1994). In

other words, no model exists that could represent the full truth, and the future is thus deeply uncertain (Keller et al., 2021; Walker et al., 2013; Lempert, 2002; Haasnoot et al., 2021). Consequently, a growing literature on decision making under deep uncertainty (DMDU) emphasizes the value of identifying decisions that are robust, in some sense, to deep uncertainties (Moody & Brown, 2013; Herman et al., 2015; McPhail et al., 2019; Borgomeo et al., 2018). Within this literature has emerged a debate regarding the value and use of probabilistic information (see Taner et al., 2019, and references therein). On the one hand, scholars have pointed out that predictions are inherently unreliable, and representing deep uncertainties through probability distributions frequently over-estimates predictive skill (Groves & Lempert, 2007; Lempert & Schlesinger, 2000). On the other, assessments of which decisions are robust depend on subjective choices about how to define robustness and how to sample uncertainties (McPhail et al., 2019; Quinn et al., 2020; Schneider, 2002, 2001; Reis & Shortridge, 2020).

In this paper we offer a conceptual step towards bridging this divide by presenting a framework that is designed to combine the strengths of both approaches. In the first step, exploratory or bottom-up modeling is used to build insight and identify potential system vulnerabilities (Moallemi, Kwakkel, et al., 2020; Bankes, 1993; Brown et al., 2012). In the second step, we synthesize the results of exploratory modeling to formally estimate performance metrics and trade-offs using probabilistic models for uncertainty. Drawing from the literature on building predictive models when all models are wrong (Box, 1976; Gelman & Shalizi, 2013; Piironen & Vehtari, 2017), we interpret these probability distributions not as statements of fact, but rather as a self-consistent framework for reasoning about how different assumptions lead to different inferences. An advantage of our approach is that it facilitates computationally efficient analysis of how alternative probabilistic models would affect estimated performance metrics and trade-offs.

We illustrate our approach through a didactic case study of whether to elevate a hypothetical house, and if so how high. Prior studies have found that floodproofing and building-scale vulnerability reduction measures, including house elevation, can effectively reduce local flood damages in many contexts (de Moel et al., 2014; de Ruig et al., 2020; Kreibich et al., 2005; Slotter et al., 2020; Rözer et al., 2016; Mobley et al., 2020; Aerts, 2018), and both local building codes (American Society of Civil Engineers, 2013; Bruneau et al., 2017; American Society of Civil Engineers, 2006) and federal policy (The Federal Emergency Management Agency, 2011) require elevation in some cases. Guidance for homeowners, notably from FEMA, recommends elevating to the base flood elevation (BFE) (typically the 100 year flood) plus a freeboard (The Federal Emergency Management Agency, 2014; ASCE, 2015; The Federal Emergency Management Agency, 2014) but recent research has demonstrated that neglecting uncertainty in the cost-benefit analysis can lead to poor decisions (Zarekarizi et al., 2020). Focusing on deep uncertainty in sea level rise (SLR) over the 70 year design life of a hypothetical house, we seek to answer the research question "*how can decision analysis transparently synthesize deep uncertainties?*" To shed light on this question in a single paper, we necessarily are silent on key issues that would be relevant to real-world decision-makers including alternative decision levers, the potential for adaptive decision rules, and rival problem framings.

We proceed as follows. In section 2 we present three formal decision analytic frameworks for analyzing an ensemble of SLR simulations, building through existing approaches for exploratory modeling scenario analysis to identify a need for synthesizing across scenarios. We present a formal framework for transparently synthesizing deep uncertainties in section 3. In section 4 we describe the didactic case study. Next, in section 5, we present results for each of the three decision lenses and discuss the advantages and limitations of each theoretical approach. In section 6 we discuss lim-

itations of the study and future research needs. Finally in section 7 we discuss key findings and implications for policy and practice.

2 Conceptual framework

In this section we introduce a conceptual framework and notation for decision analysis under deep uncertainty. We then apply this framework to understand exploratory modeling (section 2.1) and scenario-conditional probabilistic analysis (section 2.2). In section 2.3 we discuss why synthesizing across multiple scenarios is necessary. In section 3 we provide a formal method for synthesizing across scenarios.

It is common in climate risk management to work with an ensemble of trajectories of climate, economic, and other key variables, which we refer to as states of the world (SOWs). Often these SOWs are computationally expensive to generate, and thus it is important to use them efficiently. Following fig. 1, we consider using J SOWs, $\mathbf{s} = \{s_1, s_2, \ldots, s_J\}$, to evaluate I candidate decisions, $\mathbf{x} = \{x_1, x_2, \ldots, x_I\}$. For each SOW $s_j \in \mathbf{s}$ and decision $x_i \in \mathbf{x}$ we use a system model f (comprised of multiple components) to calculate a set of metrics describing the performance of decision x_i on SOW s_j, which we denote $u_{ij} = f(x_i, s_j)$. While we assume for simplicity that the decision space is known and finite, this approach could be coupled to a policy search model that proposes candidate decisions.

2.1 Exploratory modeling

A first analytical step is to use the model in an "exploratory" mode. Exploratory modeling strives to avoid making explicit assumptions about the likelihood of different SOWs and instead seeks to generate new knowledge (Bankes, 1993) by systematically exploring a large number of possible futures, emphasizing interactions between different uncertainties (Reed et al., 2022). Exploratory modeling is often paired with analyses that identify relevant scenarios (Lamontagne et al., 2018; Groves & Lempert, 2007) or summarize a system's response to forcing (Poff et al., 2015; Steinschneider et al., 2015; Sriver et al., 2018). Despite the aversion to strong assumptions about the likelihood of different futures, subjective modeling decisions such as the choice of system model, the set of candidate decisions, the criteria used to assess outcomes, and the choice of how to sample SOWs can strongly influence results (Quinn et al., 2020, 2017; Moallemi, Zare, et al., 2020).

2.2 Scenario-conditional probabilistic analysis

Although exploratory modeling is a useful framework for understanding systems, there are many questions that it cannot answer. For example, answering questions like "what is the 95th percentile of metric u under decision x" or "what is the probability of exceeding a critical threshold" requires an implicit or explicit probability distribution over outcomes (see Schneider, 2002, for a general discussion).

One way to interpret an ensemble of SOWs is as iid draws from some probabilistic data generating process. This commonly arises when a single deep uncertainty (*e.g.*, an emissions pathway) is used as an input for a stochastic model. We illustrate this concept in boxes (d) and (e) of fig. 1, denoting the particular scenario M_k. By treating the SOWs as independent and identically distributed (IID) draws from M_k, the set of outcomes $u_{i,j}$ can be interpreted as IID draws from the conditional distribution over outcomes, $p(u|x_i, M_k)$. This "scenario-conditional" probabilistic interpretation of SOWs allows for fully probabilistic quantification of uncertainty and optimization, conditional on a particular scenario. For example, S. Fletcher, Lickley, and Strzepek (2019) uses stochastic dynamic programming to quantify the value of flexibility in water resources planning. However, only a single representative concentration pathway

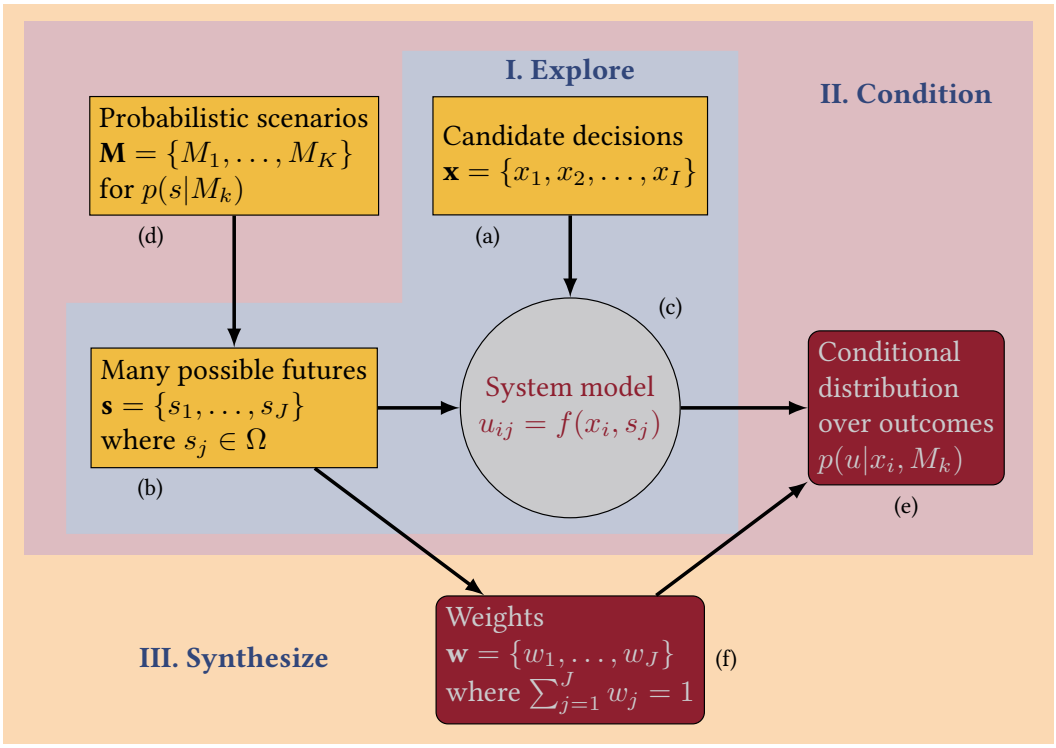

Figure 1. Outline of the proposed decision-analytic framework. In section 2.1 we use an exploratory framework to quantify the performance of candidate decisions under a large ensemble of possible futures. In section 2.2 we illustrate the "multiple PDF problem" by creating probability distributions over outcomes that are conditional upon specific probabilistic scenarios. In our case study, these scenarios correspond to combinations of emissions pathways with physical models for sea level rise. Then in section 2.3 we describe the need for synthesizing insight across scenarios. Finally in section 3 we provide a formal framework for doing so.

(RCP) scenario (RCP 8.5) is used. While the analysis could be repeated for other RCP scenarios, the scenario-conditional analysis framework only qualitatively characterize uncertainty *between* scenarios (Wong & Keller, 2017; Ruckert et al., 2019; Sharma et al., 2021).

We can also characterize DMDU methods that sample a set of parameters from fixed ranges as scenario-conditional analyses. For example, Sriver et al. (2018) sample parameters describing the rate of SLR across a range of values to inform coastal adaptation. Similarly, Trindade et al. (2020) checks the performance of candidate decisions against an ensemble of synthetic time series of streamflow, water demand, and other parameters by sampling parameters that transform the available data over a plausible range. Analyses that use this methodology are implicitly assuming a single probabilistic model in which different variables are drawn from independent Uniform distributions. Many limitations of Uniform and other noninformative priors have been documented in the literature, including (i) that they can induce unrealistic implicit priors over functions of parameters and (ii) results are sensitive to the parameterization of a given process (Seaman et al., 2012). Yet while replacing Uniform distributions with alternatives such as maximum-entropy distributions can address some of these challenges (*e.g.*, Gupta et al., 2022), subjective modeling choices remain necessary. Our primary concern here is not that these subjective modeling assumptions are wrong – this is, almost surely, inevitable – but that when these assumptions are opaque and presented without critique or validation (see Gelman et al., 2020, regarding the importance of iterative critique) they may lead to inscrutable decision processes and poor decisions.

2.3 Synthesizing deep uncertainties for decision analysis

Scenario-conditional probabilistic analysis allows for uncertainty quantification and optimization, and is valuable in many copntexts. However, scenarios are often explicitly provided without probabilities or likelihoods (*e.g.*, the shared socio-economic pathways van Vuuren et al., 2008). Thus, any such analysis is silent on the question of how to combine information across different scenarios. We term this the "multiple PDF problem". Decision making around the multiple PDF problem is susceptible to the cognitive biases that interfere with decision-making under uncertainty more generally (Tversky & Kahneman, 1974; Morgan, 1990; Srikrishnan et al., 2022). For example, while many analyses treat all scenarios as equally likely, this is often inconsistent with available information and can lead to poor decisions and outcomes (Wigley & Raper, 2001; E. Ho et al., 2019; Hausfather & Peters, 2020). Other analyses suggest using the worst-case scenario as a conservative measure. However, this approach is also problematic, since (i) there are no fundamental limits on what constitutes a worst-case scenario and (ii) improving performance under unlikely worst-case scenarios may lead to substantially impaired performance under more likely scenarios, which may or may not be acceptable to relevant stakeholders. There is thus a critical need for synthesizing insights across multiple probabilistic scenarios.

3 Re-weighting SOWs to synthesize across scenarios

In this section we provide a formal method for synthesizing across multiple scenarios to inform climate risk management. Our objective is to develop a framework that (i) is conceptually and practically amenable to exploratory modeling; (ii) makes subjective modeling choices explicit and transparent; and (iii) allows decision analysts to estimate a probability distribution over outcomes.

A particular need is to estimate the expectation of functions over SOWs (*i.e.*, box e in fig. 1). If the J SOWs are drawn IID from some distribution that credibly represents the true likelihood of different futures then the expected value of such a

function, $f(\mathbf{s})$, can be readily approximated using the Monte Carlo estimate $\mathbb{E}[f(\mathbf{s})] \approx \frac{1}{N}\sum_{j=1}^{N} f(\mathbf{s}_j)$. However, this is often not the case. For example, in section 4 we will consider decision analysis where the SOWs are sampled from multiple physical models and RCP scenarios, considering that not all RCP scenarios are equally likely and that not all physical models are equally skillful. In this case, the formula may be adjusted to a weighted Monte Carlo estimate:

$$\mathbb{E}[f(\mathbf{s})] \approx \sum_{i=j}^{N} w_j f(\mathbf{s}_j), \tag{1}$$

where $\sum_{j=1}^{J} w_j = 1$.

The challenge then becomes to suitably estimate the w_j. Many such methods exist; drawing from joint probability methods for statistical analysis of tropical cyclones, we employ a grid-based approach (Johnson et al., 2013; Resio, 2007; Toro et al., 2010). First, we project the SOWs $\mathbf{s} \in \Omega$ onto a low-dimensional representation, which we denote $\{\psi_1, \psi_2, \ldots, \psi_J\} \in \Psi$. Then, we partition the parameter space into a region corresponding to each SOW and integrating the probability $p(\psi)$ over each region.

Doing so requires a probabilistic model for this low-dimensional representation of the SOWs, $p(\psi)$. We denote this model p_{belief} to emphasize that it represents a subjective belief about the SOWs, rather than an objectively verifiable choice. In general we do not expect that stakeholders and experts will agree on p_{belief} because there is not, even conceptually, an objectively correct choice (Oreskes et al., 1994; Walker et al., 2013). However, we posit that since we cannot be "right," it is valuable to maximize the transparency of our implicit probabilistic assumptions, and suggest that writing down an explicit model for p_{belief} supports this aim. Choices for p_{belief} can be drawn from many sources, including expert elicitation or results of previous analyses. These models can be interpreted as prior beliefs about SLR that could be incorporated into a Bayesian analysis as additional data is collected in the future, and thus can draw from literature on Bayesian prior selection and prior predictive checks (Gelman et al., 2020).

We present here the case where the ψ_j are one-dimensional; extensions to higher dimensions are possible. We first sort the ψ_j from least to greatest so that $\psi_{j-1} \leq \psi_j$, $(j \neq 1)$. Defining a cumulative distribution function $F_{\text{belief}}(\psi) = \int_{-\infty}^{\psi} p_{\text{belief}}(\psi')\,\mathrm{d}\psi'$, we calculate weights as

$$w_j = \begin{cases} F_{\text{belief}}\left(\frac{\psi_1+\psi_2}{2}\right) & j = 1 \\ F_{\text{belief}}\left(\frac{\psi_j+\psi_{j+1}}{2}\right) - F_{\text{belief}}\left(\frac{\psi_{j-1}+\psi_j}{2}\right) & 1 < j < J \\ 1 - F_{\text{belief}}\left(\frac{\psi_{J-1}+\psi_J}{2}\right) & j = J. \end{cases} \tag{2}$$

This step is illustrated in fig. 2. By the definition of cumulative distribution functions, $F_{\text{belief}}(b) - F_{\text{belief}}(a) = \int_a^b p_{\text{belief}}(\psi')\,\mathrm{d}\psi'$. Diagnostic checks, such as examining the histogram of weights to (not shown), may be useful protections against degeneracy.

The aim of this re-weighting framework is to integrate an ensemble of SOWs used for exploratory modeling into formal decision analysis, even when the SOWs deliberately over- or under-sample some regions of the parameter space. As in section 2.2, we must condition on a model: where the analysis of section 2.2 conditions upon deep uncertainties, the approach outlined in this subsection synthesizes across them. Considering multiple probabilistic models for p_{belief} can also be useful for understanding the sensitivity of the decision to the choice of p_{belief}. Further, the sensitivity, or lack thereof, of different objectives to the choice of p_{belief} may be useful for identifying future research needs.

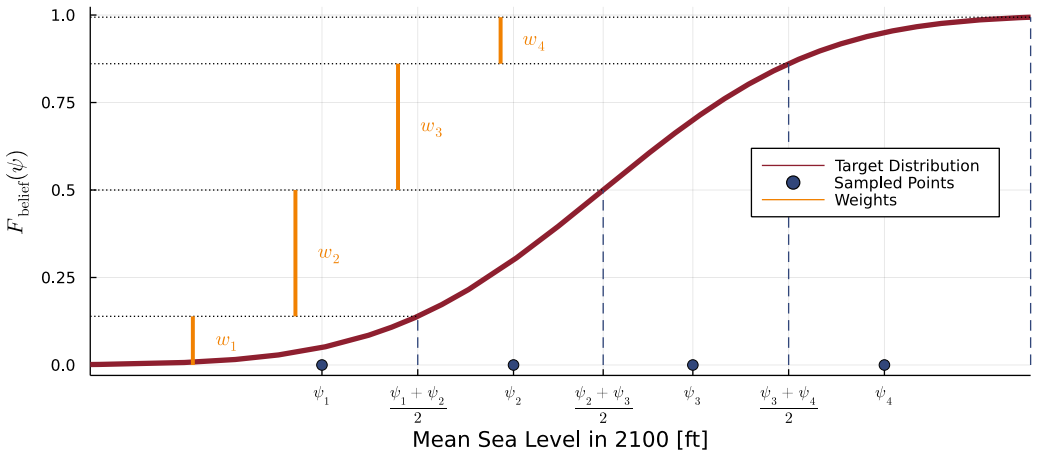

Figure 2. Schematic of SOW re-weighting scheme defined in eq. (2). This method is illustrated for a hypothetical target distribution (dark red line) and $J = 4$ samples $\psi_1, \psi_2, \psi_3, \psi_4$ (blue dots). As shown in eq. (2), the weights w_j (orange vertical lines) are calculated based on the cumulative distribution function of the target distribution at the halfway points $\frac{1}{2}[\psi_j + \psi_{j+1}]$ (vertical dashed lines).

4 Demonstrating the concept with a case study

To illustrate the proposed decision analytic framework, we model a one-time decision of whether to elevate a house, and if so by how much (fig. 3). Following the approach outlined in Zarekarizi et al. (2020), we focus on a case study of a *hypothetical* house in Norfolk, VA. For interpretability, we focus on deep uncertainty in mean relative sea level (MSL) and treat storm surge and other model parameters as shallow uncertainties as shown in table 1. We use the notation developed in the previous section to describe the case study. Specifically,

1. The decision vector $\mathbf{x}$ is comprised of discrete possible house heightenings (Δh); we consider $\Delta h = \{0\,\text{ft}, 0.25\,\text{ft}, \ldots, 12\,\text{ft}\}$.
2. The SOWs describe annual time series of MSL over the $T = 70$ year house lifetime so $\mathbf{s} \in \mathbb{R}^T$
3. The system model f quantifies up-front costs (the cost of elevating) and lifetime expected damages (the structural cost of experiencing floods), given a decision x_i and SOW s_j, by integrating economic and engineering damage models over a probability distribution for storm surge. We elaborate upon these metrics in section 4.3.

In the remainder of this section we describe data sources and treatment of SLR (section 4.1), storm surge (section 4.2), damages and metrics (section 4.3), and finally the subjective probabilistic models p_{belief} used to apply the re-weighting method described in section 2.3 to this case study (section 4.4).

4.1 Sea level rise

We analyze simulations of MSL at Sewells Point, VA from four probabilistic physical models using data published in Ruckert et al. (2019). The four models considered are (i) the BRICK model (version 0.2) with slow ("BRICK Slow") and (ii) fast ("BRICK Fast") ice sheet dynamics (Wong et al., 2017), (iii) the Kopp et al.

Table 1. Summary of parameters, their notation, and how their uncertainty is represented. Symbols describing the decision-analytic framework are described in fig. 1.

Name	Symbol	Uncertainty
MSL	$\overline{y}(t)$	Deeply uncertain: four physical models × four RCP scenarios
Storm surge	$y'(t)$	Probabilistic: Bayesian inference on a stationary GEV model
Annual maximum flood	$y(t)$	Deterministic: $y(t) = \overline{y}(t) + y'(t)$
Discount rate	ρ	Determinitic: 2.5% per year
Depth-damage	$D(h - y)$	Deterministic: based on HAZUS model (see Zarekarizi et al., 2020)
Elevation cost	$C(\Delta h)$	Deterministic: a piecewise linear model following Zarekarizi et al. (2020)
Initial height	h_0	Deterministic: 1 ft below the BFE, unless otherwise noted
House floor area	–	Deterministic: 1500 ft^2
Structural value	–	Deterministic: \$200 000
House lifespan	T	Deterministic: 70 years

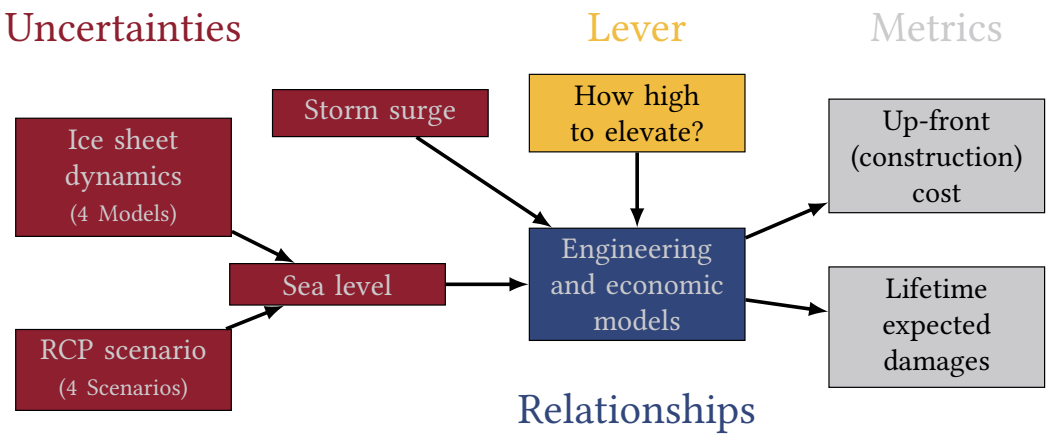

Figure 3. Conceptual diagram of the considered example. A state of the world (SOW) consists of a description of the uncertain factors (red). We model a problem with a single lever (yellow), which is how high to elevate a house (Δh). For each SOW (red) and each value of Δh, the system model (blue) is used to calculate performance metrics (gray). We also compute a third metric, expected lifetime costs, which is the sum of up-front costs and lifetime expected damages.

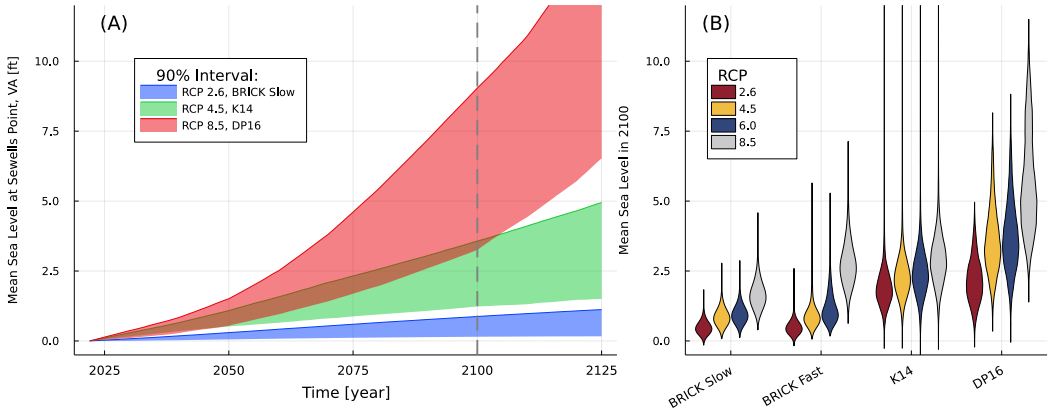

Figure 4. Projections of future mean sea level depend strongly on the choices of physical model and forcing. (A): 90% confidence intervals for mean sea level at Sewells Point, VA as a function of time for a representative subset of three probabilistic models (out of sixteen). (B): probability distribution of MSL at Sewells Point, VA in the year 2100 for each probabilistic model considered.

(2014) model ("K14"), and (iv) the DeConto and Pollard (2016) model ("DP16"). The Kopp et al. (2014) and DeConto and Pollard (2016) models have a ten year time step, which we linearly interpolate onto a one year time step for consistency. Estimates of nonstationary MSL also depend on anthropogenic forcing, which is itself deeply uncertain (E. Ho et al., 2019; Srikrishnan et al., 2022). To sample this uncertainty, we use simulations from each physical model under four RCP scenarios, yielding sixteen time-varying probabilistic scenarios of MSL.

The choices of physical model and RCP scenario jointly determine future MSL $p(\overline{y}|t)$. Figure 4(a) shows the time-varying 90% credible intervals of MSL for three representative models. The divergence between the the best-case (blue) and worst-case (red) models is small in the early 21st century and increases rapidly thereafter. Figure 4(b) shows the PDFs of mean sea level in 2100 (dashed vertical line in panel (a)) under each of the sixteen probabilistic scenarios considered. The stark differences between different scenarios of SLR arise primarily from different representations of Antarctic Ice Sheet contributions to global SLR and statistical calibration methodologies. For a more detailed discussion we refer the reader to Ruckert et al. (2019). We return in section 5.2 to the challenge of decision making given multiple PDFs.

4.2 Storm surges

Following prior work (*e.g.*, Garner & Keller, 2018; Sriver et al., 2018), we model annual maximum floods $y(t)$ as the sum of sea level $\overline{y}(t)$, described in the previous subsection, and annual maximum storm surges $y'(t)$, neglecting any potential hydrodynamic interactions.

We use data on storm surge at Sewells Point, VA (gauge 8638610) from the NOAA tides and currents data archive (National Oceanographic and Atmospheric Administration, 2022). Hourly recordings of water level are available from 1928 to the present; we use data from the period January 1, 1928 to December 31, 2021. For each calendar year we first remove the annual mean, then calculate the maximum water level. We refer this time series of annual maximum storm surges as $y'(t)$. We display this time series of annual maxima storm surges in fig. 5(a). The largest recorded surge

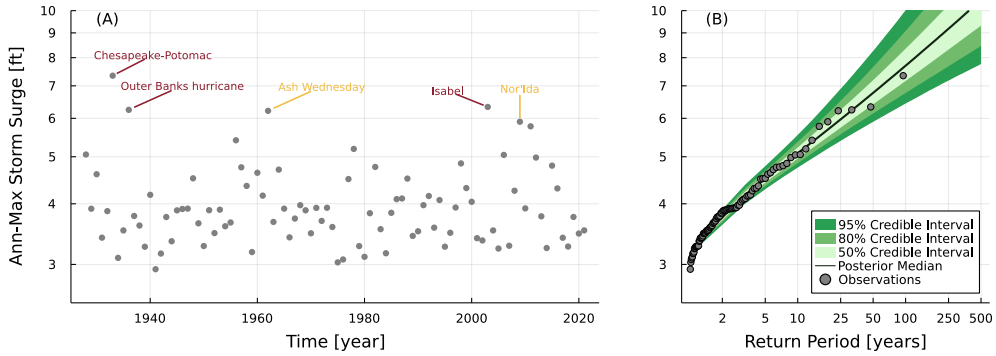

Figure 5. Annual maximum storm surges (after subtracting mean relative sea level) at Sewells Point, VA from the freely available NOAA tides and currents data archive (National Oceanographic and Atmospheric Administration, 2022). (A): time series of historic storms. Red (yellow) arrows denote notable tropical cyclones (Nor'easters). (B): return periods. Dots indicate observed values; their x-value is their plotting position using the Weibull formula (eq. S5). Gray lines show the 50, 80, and 95% posterior confidence intervals from the Bayesian GEV fit (section 4.2).

was the Chesapeake-Potomac hurricane of 1933, which caused a surge of over 7 ft at this gauge, but other hurricanes and Nor'easters have caused surges above 6 ft.

We model future storm surge using a stationary GEV model:

$$y'(t) \sim \mathrm{GEV}(\mu, \sigma, \xi), \tag{3}$$

where $y'(t)$ is the storm surge (above MSL) in year t and a GEV distribution with location, shape, and scale parameters μ, σ, and ξ, respectively, has the probability density function given in eq. (S1). This model assumes stationarity, neglecting any potential time dependence.

Our approach to model assessment is based on the concept of principled workflow design for model building and checking (see Gelman et al., 2020, for details). One model choice, analogous to the choice of statistical distribution or the assumption of stationarity, is the choice of how to represent prior information. We include two forms of prior information. First, we constrain the shape parameter to be positive, $\xi > 0$, to reflect knowledge about the support of y', which for a variable distributed according to eq. S1 is:

$$\text{supp } y' = \begin{cases} \xi < 0: & y' \in (-\infty,\ \mu - \sigma/\xi) \\ \xi > 0: & y' \in (\mu - \sigma/\xi,\ \infty). \end{cases}$$

Since storm surges cannot be negative, only the latter is physically defensible, justifying our choice to constrain the shape parameter to be positive. Second, we add weakly informative priors. Rather than applying prior information directly over the joint distribution of the parameters $\{\mu, \sigma, \xi\}$, we instead apply a prior over extreme quantiles of the distribution, as in Coles and Tawn (1996). Specifically, we apply Inverse Gamma priors over the 2, 10, 100, and 500 year return levels, with means of 4 ft, 6 ft, 10 ft and 15 ft and standard deviations of 1.5 ft, 1.75 ft, 2.25 ft and 2.75 ft, respectively. The parameters of the Inverse Gamma distribution can be calculated from these moments (see eq. S3). These means and standard deviations were chosen to represent plausible physical ranges (fig. S4).

For inference, we draw 10 000 samples from the posterior distribution $p(\mu, \sigma, \xi | y')$ using Hamiltonian Markov Chain Monte Carlo (Betancourt, 2018; Hoffman & Gelman,

2011) implemented in the Turing package of the Julia programming language (Perkel, 2019; Ge et al., 2018; Tarek et al., 2020; Besançon et al., 2021; Bezanson et al., 2012). Diagnostics suggest (though cannot guarantee) convergence (see table S1). We evaluate the model's fit using posterior predictive checks (see Gelman et al., 2020, section 2.4 and references therein). Using the lag 1 and 2 partial autocorrelations, sample maximum, sample minimum, sample median, and Mann-Kendall test value as Bayesian test statistics, we find that draws from the posterior predictive distribution match the observed test statistics credibly (fig. S9) although panels (a) and (b) suggest the possibility of temporal structure not captured by our stationary IID model. Future efforts could represent this structure by conditioning the parameters of the distribution on relevant climate indices (as in Wong, 2018; Farnham et al., 2018, 2017; Ossandón et al., 2021).

Other model validations lend confidence to the stationary GEV model selected. For example, fig. 5(b) shows the estimated return periods for these storm surges; the estimated return period (shading) matches the the empirical plotting position (dots) and a positive control test (fig. S6) validates the model's ability to recover known parameter values.

4.3 Damages and metrics

The system model ("relationships" in fig. 3) is comprised of two key pieces. The first is a fragility model that estimates the expected flood damages for a particular year ("expected annual damages"), given the elevation of the house and the mean sea level for that year. The second model converts a time series of annual expected damages into lifetime expected damages.

We define expected annual damages in year t as the expectation of the damage function with respect to storm surge. This expectation depends on the house's height ($h = h_0 + \Delta h$) where h_0 is the initial height relative to the gauge and Δh is the amount by which the house is elevated. The expected annual damage is thus

$$\mathrm{EAD}(t) = \mathbb{E}[D(h - \overline{y}(t))] = \int_{y'} p(y') D(h - (\overline{y}(t) + y')) \, \mathrm{d}y' \,, \tag{4}$$

where $D(h - y)$ is a deterministic function specifying damage as a function of flood depth (relative to the house) and $p(y')$ is the probability density of storm surge. Following Zarekarizi et al. (2020), we use the Hazard U.S. (HAZUS) depth-damage curves provided by FEMA; this depth-damage relationship is shown in fig. S1. For comparison, fig. S1 also shows the "Europa" depth-damage relationship developed by the Joint Research Center of the European Commission's science and knowledge service (Huizinga & Szewczyk, 2016). Both models show damage increasing with flood depth before reaching an upper limit but differ in the value of the upper limit and the rate at which damages approach it. Although Zarekarizi et al. (2020) demonstrate that the choice of fragility function is important for informing house elevation, we use only the HAZUS model for simplicity.

The expected annual damage is sometimes calculated by assuming analytically tractable functional forms for the depth-damage relationship and for the distribution of hazard (*e.g.*, van Dantzig, 1956). However, the convolution of the HAZUS depth-damage equation with the GEV posterior does not have a tractable analytic solution. Instead, we estimate this convolution through a Monte Carlo method (see section S1.2 for details). Then, because the expectation in eq. (4) depends only on $h - \overline{y}(t)$, we calculate expected annual damages for a wide range of possible heights, then use this to train a computationally efficient surrogate model (using linear interpolation; see section S1.3).

The second component of the system model converts a time series of EAD into lifetime expected damages, which we define as the up-front discounted sum of expected annual damages:

$$\text{LED} = \sum_{t=t_i}^{t_f} \gamma^{(t-t_i)} \text{EAD}(t), \tag{5}$$

where $\gamma = 1 - \rho$ (ρ being the discount rate), the initial time $t_i = 2022$, and the end time $t_f = t_i + T - 1$. Although Zarekarizi et al. (2020) show that uncertainty in the discount rate is important for decision support, we use a fixed discount rate (see table 1) for the purposes of this didactic study. For a more theoretical discussion see Arrow et al. (2013).

To assess the performance of a given decision for a specific SOW ("Metrics" in fig. 3), we calculate the following metrics for each decision-SOW combination:

1. "Up-front cost" is the cost of elevating a house. Following Zarekarizi et al. (2020), we use estimates of construction cost from the Coastal Louisiana Risk Assessment (Fischbach et al., 2012). We normalize this cost by house value; this cost curve is shown in fig. S3 and shows a large up-front cost plus a piecewise linear marginal cost.
2. "Lifetime expected damages" is calculated following eq. (5).
3. "Expected lifetime costs" is the sum of lifetime expected damages and up-front costs.

4.4 Prior over sea level rise

We construct three probabilistic models for $p_{\text{belief}}(\psi)$, which represents the amount of SLR from 2022 to 2100.

We use a Gamma distribution for all three priors, parameterized following eq. (S4). The distributions were chosen to be illustrative, rather than to reflect any particular scientific consensus. The Gamma distribution is a flexible distribution that can be used to model skewed, lower-bounded distributions, making it an appropriate choice for modeling subjective uncertainty about SLR. Table 2 specifies the parameters of these distributions, as well as some quantiles of the distributions. Their PDFs are also plotted in fig. 8(A).

Table 2. Subjective probability distributions over SLR from 2022 to 2100, *i.e.* $p_{\text{belief}}(\psi)$. The name of the distribution, the parameters of the Gamma distribution with shape α and scale θ, and the 2.5, 25, 50, 75, and 97.5th percentiles (values in ft).

Name	Parameters		Percentiles (in ft)				
	α	θ	2.5	25.0	50.0	75.0	97.5
Slow SLR	1.75	0.50	0.08	0.39	0.72	1.19	2.57
Uncertain SLR	1.75	1.25	0.21	0.98	1.79	2.97	6.41
Rapid SLR	3.50	1.25	1.06	2.66	3.97	5.65	10.01

We developed these priors for didactic purposes, to illustrate a range of possible beliefs. We can compare them, for example, with analysis published by NOAA, which project 1.94 ft, 2.62 ft, 4.27 ft, 5.25 ft and 6.89 ft for the low, intermediate, low intermediate, intermediate high, and high scenarios, respectively (Sweet et al., 2022, table. 2.4). We can also compare to the analyses of Sriver et al. (2018) which uses a

rescaled Beta distribution with bounds of 0.83 ft to 8.2 ft and a most plausible estimate of 3.1 ft. Our samples bound all of these estimates.

5 Results and discussion

We illustrate our approach to synthesizing uncertainties by sequentially analyzing the house elevation problem through multiple lenses for DMDU. This allows us to demonstrate the advantages and limitations of each approach, and to highlight the value of synthesizing across multiple scenarios.

5.1 Exploratory modeling

We begin by using our model in an "exploratory" mode with an aim of learning about interactions between system dynamics and decisions.

One application of exploratory analysis is to reveal the range and variation in outcomes, conditional on taking a particular decision. Figure 6 shows the dependence of expected lifetime costs (damages plus up-front costs; y-axis) as a function of SLR over the house lifetime (x-axis), height increase (Δh; columns), and initial elevation (h_0; rows). The outcomes with lowest total lifetime costs arise when the house is not elevated ($\Delta h = 0$) and SLR is minimal (bottom left corners). The outcomes with highest total lifetime costs arise when the house is elevated only slightly and SLR is rapid. As Δh increases, the best-case scenario becomes more expensive because up-front costs increase, but worst-case scenarios become less expensive because even if SLR is substantial, damages will be negligible.

This analysis answers "what-if" questions like "given h_0 and Δh, what is the range of total costs a homeowner could face if SLR over the house lifetime is 1 ft or 10 ft." For some decision-makers, contextualizing this information against a few scenarios of SLR (*e.g.*, those of Sweet et al., 2022) may prove sufficient for decision making. However, this analysis is silent on how to estimate cost-benefit comparisons, return periods, and other trade-offs.

5.2 Scenario-conditional probabilistic analysis

We now turn to the scenario-conditional analysis described in section 2.2. Whereas the exploratory analysis of the previous subsection interpreted each time series of future sea level as a sample from the space of possible futures, we can also interpret each SOW as a draw from one of the sixteen probabilistic scenarios of SLR shown in fig. 4. As discussed in section 2.2, this allows a formal estimation of decision metrics, conditional on the chosen scenario.

As discussed in section 2.2, this probabilistic interpretation allows us to compute expected values of functions. For example, fig. 7(a) plots the expected total lifetime cost as a function of Δh for the sixteen probabilistic scenarios considered (we highlight three representative models). This panel shows lifetime expected damages as a function of Δh, shown in fig. 7(b, plus the up-front cost of construction. Because there are high fixed costs associated with building (see cost curve in fig. S3), it generally does not make sense to raise the house by only a small amount, since this incurs these fixed costs without providing substantial damage reduction. Figure 7 shows that estimates of trade-offs between up-front cost and expected lifetime costs are highly sensitive to the chosen scenario. For small Δh, expected costs are low under optimistic scenarios (*e.g.*, RCP 2.6 with slow ice sheet dynamics; red lines) and high under pessimistic scenarios (*e.g.*, RCP8.5 with the DP16 model; blue lines). Estimates of the optimal decision are highly sensitive to the choice of scenario. For example, under the most pessimistic scenario (blue line), the cost-minimizing height increase is 6 ft, which incurs

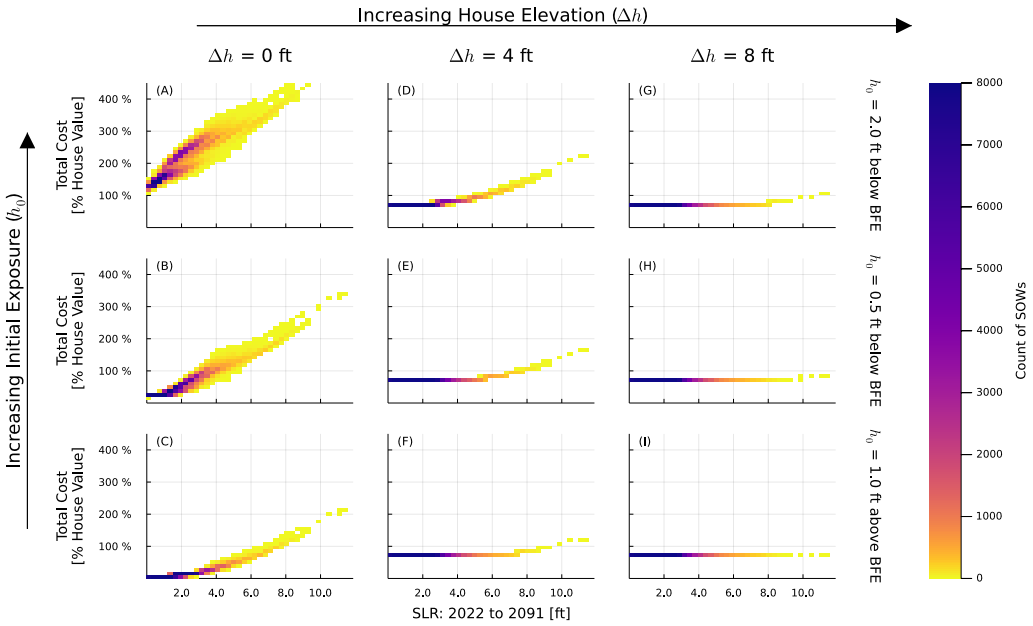

Figure 6. Scenario maps show the dependence of expected lifetime cost (damages plus up-front cost) as a function of mean relative sea level (MSL) in 2100 for several values of initial height (h_0) and house elevation (Δh). Colors indicate the number of states of the world (SOWs) of falling within each box. The lowest-cost outcomes occur when exposure is low (h_0 is large and sea level rise (SLR) is minimal) and the house is not elevated (no up-front cost). The highest-cost outcomes arise when exposure is high (h_0 is small and SLR is rapid) and investment is inadequate. In all cases, elevating the house reduces the variance in total lifetime cost. Values are sensitive to model constants; see table 1.

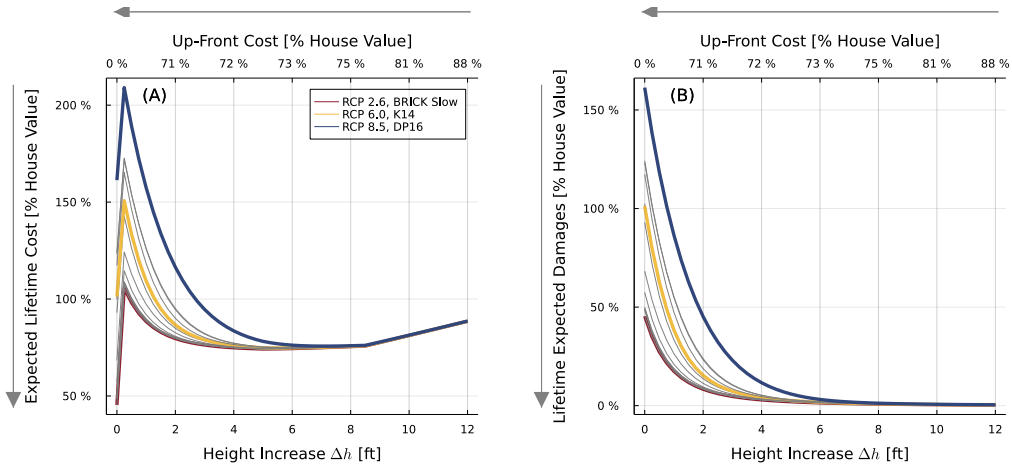

Figure 7. Each probabilistic model or scenario leads to a different estimate of the Pareto frontier. For emphasis, we highlight three representative models: the Brick Slow model (Wong et al., 2017) under RCP 2.6, the K14 (Kopp et al., 2014) model under RCP 6.0 and the DP16 model (DeConto & Pollard, 2016; Kopp et al., 2017) under RCP 8.5. (A): trade-off between up-front cost (which is a monotonic function of height increase) and expected lifetime costs. (B): trade-off between up-front cost and lifetime expected damages (eq. 5). Light gray lines show estimates for all 16 models (four RCP scenarios times four physical parameterizations) considered. Colored lines highlight three representative models for emphasis. The gray arrows indicate the direction of preference.

an up-front cost of 73% of the house value but reduces lifetime expected damages by over 150% of house value. Under the most optimistic scenario (gray line), the cost-minimizing decision is to not elevate, as elevating 6 ft incurs the same up-front cost yet reduces lifetime expected damages by less than 50% of house value.

This approach is, in a sense, another form of exploratory modeling: instead of considering a very large ensemble of SOWs, we consider a much smaller set of probabilistic models. Scenario-conditional analysis can be attractive because it allows modelers to focus on their domain expertise (*e.g.*, the response of ice sheets and global sea levels to a particular climate future). However, conditioning simulations on a set of climate futures and physical models presents what we term "the multiple PDF problem" because it leaves decision makers with many PDFs to choose from and hence many trade-off curves to navigate. The multiple PDF problem has also been discussed in other contexts. For example, Sharma et al. (2021) model the reliability of stormwater infrastructure under different climate models and downscaling methods, finding diverging estimates of future rainfall hazard, even under a single RCP scenario. Similarly, Wong and Keller (2017) construct 18 probability distribution functions for future flood risk in New Orleans, considering multiple models for ice sheet dynamics and storm surge and multiple RCP scenarios. As a last example, Haasnoot et al. (2021) identify global adaptation needs for different SLR scenarios. Although this scenario-conditional analysis is appropriate for understanding differences between models, its key limitation is that it **places the burden for deciding which model to design for onto the end user.** Since not all house owners or contractors have expertise in assessing the relative likelihood of different climate futures, they may not be well positioned to make this decision.

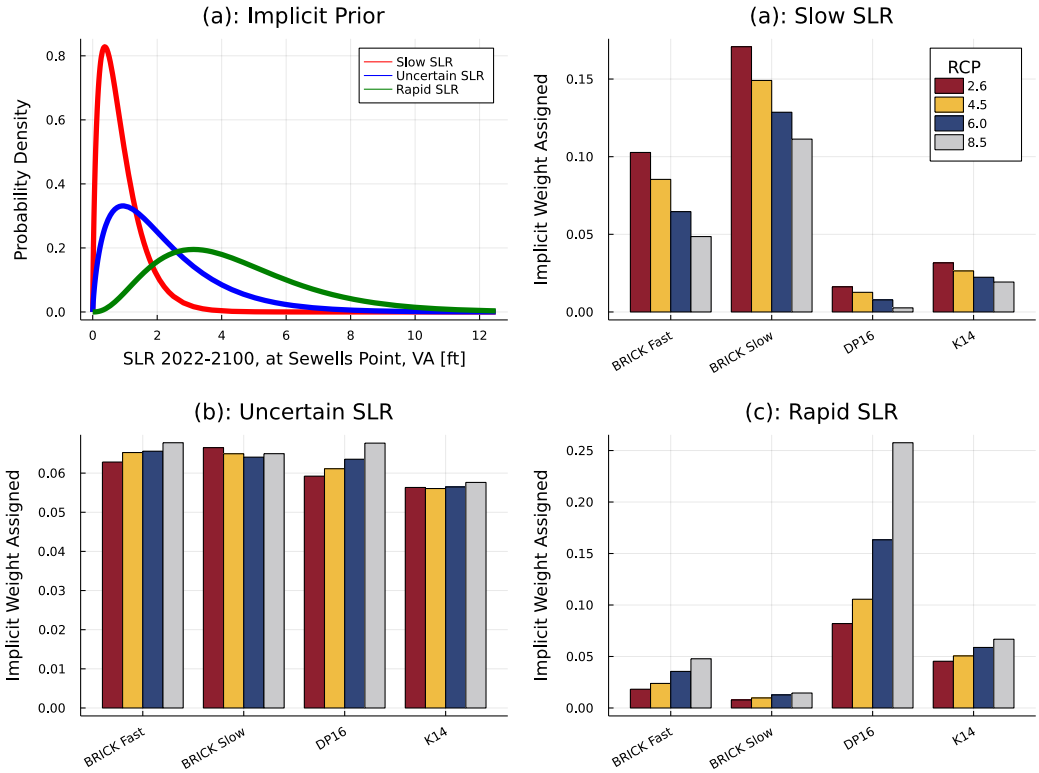

Figure 8. Impact of different subjective probability distributions for local sea level on implicit weight given to each RCP scenario and physical model. We develop three distributions representing plausible probabilistic beliefs (p_{belief}) over MSL at Sewells Point, VA in 2100, relative to the present. The PDFs of these distributions are shown in panel (A). In panels (B-C) we show the relationship between these distributions and the 16 probabilistic models (four RCP scenarios and four physical representations) available. Specifically, (B-C) show the average weight given to each model by each choice for p_{belief}.

5.3 Synthesizing deep uncertainties for decision analysis

The SOW re-weighting framework described in section 3 can help overcome the limitations of scenario-conditional analysis. In this section we illustrate how this approach can help to shed light on climate risk management under deep uncertainty. We present results using each of the models for p_{belief} outlined in section 4.4; these three distributions are shown in fig. 8(A).

One application of this method is to diagnose the assumptions which which different p_{belief} are consistent. Figure 8(B-D) shows the total weight that each choice of p_{belief} assigns to SOWs generated by each RCP scenario and physical model. Specifically, weights are computed as the sum of weights assigned to each SOW sampled from that model. For example, the rapid SLR scenario (green line in fig. 8) places most weight on SOWs produced by the DP16 model, and particularly on RCP 8.5 which by some accounts is unlikely given current policy (Hausfather & Peters, 2020; Srikrishnan et al., 2022). Conversely, the slow SLR scenario (red line) places most weight on the BRICK models, particularly RCP 2.6 (also unlikely given current policy; Hausfather & Peters, 2020; Srikrishnan et al., 2022) and RCP 4.5. The uncertain SLR scenario (blue line) allocates approximately equal weight across models. Decision analysts can use

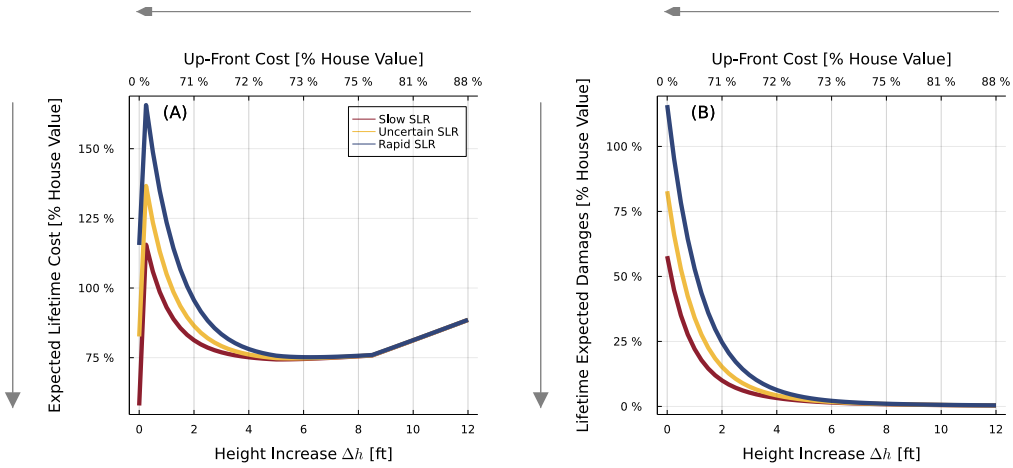

Figure 9. As fig. 7, but with Pareto frontiers for the full distribution of outcomes using the three models of p_{belief} (colors).

this approach as a diagnostic to understand the assumptions implicit to their choice of p_{belief}.

This method can also be used to calculate expectations, allowing us to revisit the trade-off diagrams of fig. 7. Figure 9 shows the total lifetime cost (panel A) and lifetime expected damages (panel B) under each choice of p_{belief}. Notably, they give different guidance. Under an assumption of rapid SLR, elevating the house by approximately 6 ft costs 73% of house value and reduces damages by over 100% of house value, yielding a benefit to cost ratio of approximately 1.25. Under an assumption of slow SLR, the same decision reduces damages only by 50% of house value, yielding a benefit to cost ratio of approximately 0.7. Under the intermediate / uncertain SLR assumption, the expected lifetime costs are similar for elevating or not elevating the house, and thus the benefit to cost ratio is nearly 1. Under all assumptions, elevating by only a few feet is impractical because it involves paying the large fixed costs of elevation (fig. S3) but offers relatively little flood reduction. Based on this analysis, we would recommend that the owner if this hypothetical home elevate by approximately 4-6ft or not at all. Alternatively, the homeowner could choose to defer the decision of whether, and how high, to elevate; our analysis did not consider this possibility but there is a rich literature on flexible design and engineering options analysis in climate risk analysis (*e.g.*, S. Fletcher, Lickley, & Strzepek, 2019; S. Fletcher, Strzepek, et al., 2019; Hui et al., 2018; Garner & Keller, 2018; Herman et al., 2020; de Neufville & Smet, 2019).

6 Limitations and research needs

Several limitations to our study merit further discussion. The first category has to do with limitations of the underlying method proposed for re-weighting SOWs. For example, we develop a subjective probabilistic model $p_{\text{belief}}(\Psi)$ over MSL in the year 2100. Although this is a low-dimensional representation of the full time series, it is not a sufficient statistic. In other words, many possible low-dimensional representations are possible and time series with the same MSL in 2100 may differ in other ways. For problems with more sources of uncertainty, such as multisector problems, choosing an appropriate low-dimensional representation may prove challenging. In such settings, diagnostics and sensitivity analyses may shed light on the appropriateness of different modeling choices. A related concern is that we developed our three distributions for

$p_{\text{belief}}(\Psi)$ in an *ad hoc* fashion that may not represent well-calibrated beliefs. Although this is appropriate for our didactic illustration, recent advances in Bayesian elicitation of expert opinion (see Mikkola et al., 2021, and references therein) can be applied to improve decision making in real world case studies. More fundamentally, our method assumes that there exists an expert capable of integrating over the many processes that drive SLR, from global greenhouse gas emissions to the global carbon cycle to climate sensitivity and ice sheet response (Morgan, 2014). An alternative approach would be to build a probabilistic model for each of these steps, and to use each as an input to the next to develop a fully probabilistic model for SLR. Yet while some progress has been made developing probabilistic models for specific elements of this model chain (*e.g.*, Srikrishnan et al., 2022; Wong et al., 2017), this remains a computational and conceptual challenge.

The second category of limitations has to do with the case study and our interpretation of the house elevation decision problem. This problem intersects with decisions about where to live and how to manage household finances, both of which are highly complex. One extension of our analysis would be to consider additional decision objectives. In particular, we hypothesize that incorporating improved representations of risk aversion into decision support may substantially improve their usability. One could also extend the analysis to consider additional sources of uncertainty such as depth-damage relationships (Rözer et al., 2019; Nofal et al., 2020), the cost of elevating a house, the house lifespan, the effective discount rate, and value of the land on which the house is built (Zarekarizi et al., 2020). Finally, while here we consider the decision to be a one-time decision, one could also frame this as a sequential decision problem. The analysis of sequential decision problems applies tools from control theory and reinforcement learning to identify policies that map "triggers" (*i.e.*, state variables) to decisions (Herman et al., 2020). Yet although framing the decision through a sequential lens can increase adaptability and improve outcomes (S. M. Fletcher et al., 2017; Garner & Keller, 2018), decisions and outcomes remain highly sensitive to the characterization of uncertainty (Herman et al., 2020), and thus the problem of synthesizing across deep uncertainties remains relevant.

These limitations motivate several directions for future research. From a methodological perspective, developing model chains that capture uncertainties in global energy and economic pathways, global climate sensitivity, and local hazard response (see fig. 1 of Moss & Schneider, 2000) offers a principled framework for fully probabilistic estimation of local hazard, subject to (still necessarily subjective) probabilistic models for key parameters. From a decision support perspective, improved understanding of the conditions under which household-scale strategies for flood risk management, like elevation, achieve relevant objectives could support improved resilience and adaptation. Additionally, since developing bespoke analyses for each house may be impractical, identifying decision rules that are applicable across different house characteristics may improve usability and guidance. Finally, there are many parallels between DMDU and subjective Bayesian literature on building predictive models in the "$\mathcal{M}$-closed" case when "all models are wrong" (Gelman & Shalizi, 2013; Box, 1976), and thus future work can demonstrate how to incorporate techniques from Bayesian workflow (see Gelman et al., 2020) into DMDU methodologies.

7 Conclusions

This study develops a framework designed to increase the transparency of quantitative decision analysis under deep uncertainty. We develop a framework capable of blending iterative, stakeholder-driven exploratory modeling (see, *e.g.*, Helgeson et al., 2022) with subjective probabilistic expert assessment. Such an approach is urgently needed given that deeply uncertain nonstationarity hazards pose a fundamental challenge to classical methods of hazard estimation. We use a didactic case study of house

elevation in the coastal zone to illustrate a method for transparently synthesizing across deep uncertainties.

The proposed SOW re-weighting framework can be applied to inform critical challenges in climate risk management. An obvious area of application is to the design of infrastructure. For example, much of the stormwater infrastructure in the United States is inadequate for current and anticipated future climates (Lopez-Cantu & Samaras, 2018). Yet upgrading this infrastructure is costly and subject to large uncertainties between rainfall models (Sharma et al., 2021) and RCP scenarios. Similarly, decisions like levee heightening (Garner & Keller, 2018; Oddo et al., 2017; van Dantzig, 1956) and sea wall design (United States Army Corps of Engineers, Galveston District & Texas General Land Office, 2021, Appendix D., p. 2-59) are subject to deep uncertainties including sea level rise. Investments in water resources planning and management also depend on assumptions of future water demand, availability, and technologies (Trindade et al., 2019). And analyses of climate change mitigation options, such as estimates of the social cost of pollutants (Errickson et al., 2021) or cost-minimizing energy transition pathways, are conditional on probabilistic models for inputs like technology prices and population.

Of course, all models are ultimately wrong (Box, 1976). Thus seeking decisions that perform well across a range of assumptions, and improving the decision space through robust design and flexibility, can improve outcomes. Yet whenever decisions are compared quantitatively, assumptions about the probability of different possible futures are necessarily made. We call for researchers studying climate risk management to make these implicit assumptions explicit, and we suggest that coordinated guidance can help practitioners determine better design criteria.

8 Open Research

All code, including source code, is available under the GNU Public License (version 3) at `https://github.com/jdossgollin/2022-elevation-robustness`. This code is written in the open source Julia programming language and detailed instructions for reproducing our results are provided. A permanent, citeable archive of the precise version of the codes used in this study is also available on Zenodo at `https://doi.org/10.5281/zenodo.6814588`.

Acknowledgments

This work was supported by the National Oceanic and Atmospheric Administration (NOAA) through the Mid-Atlantic Regional Integrated Sciences and Assessments (MARISA) program under NOAA grant NA16OAR4310179 and through the Penn State Initiative for Resilient Communities (PSIRC) by a Strategic Plan seed grant from the Penn State Office of the Provost, with co-support from the Center for Climate Risk Management (CLIMA), the Rock Ethics Institute, Penn State Law, and the Hamer Center for Community Design. JDG thanks Rice University for support. KK thanks Dartmouth College for support. The authors thank Sitara Baboolal, Courtney Cooper, Tor Erlend Fjelde, Catalina González-Dueñas, Adam Pollack, Vivek Srikrishnan, Skip Wishbone, and two anonymous peer reviewers for helpful comments that improved this research.

References

Aerts, J. C. J. H. (2018, November). A Review of Cost Estimates for Flood Adaptation. *Water*, *10*(11), 1646. doi: 10.3390/w10111646

American Society of Civil Engineers. (2006). *Flood resistant design and construction.*

Reston, VA: Author.
American Society of Civil Engineers. (2013). *Minimum design loads for buildings and other structures*. Author. doi: 10.1061/9780784412916
Arrow, K., Cropper, M., Gollier, C., Groom, B., Heal, G., Newell, R., … Weitzman, M. (2013, July). Determining benefits and costs for future generations. *Science*, *341*(6144), 349–350. doi: 10.1126/science.1235665
ASCE. (2015). *Flood resistant design and construction*. Reston, VA: American Society of Civil Engineers.
Bankes, S. (1993, June). Exploratory modeling for policy analysis. *Operations Research*, *41*(3), 435–449. doi: 10.1287/opre.41.3.435
Besançon, M., Papamarkou, T., Anthoff, D., Arslan, A., Byrne, S., Lin, D., & Pearson, J. (2021). Distributions.jl: Definition and Modeling of Probability Distributions in the JuliaStats Ecosystem. *Journal of Statistical Software*, *98*(16). doi: 10.18637/jss.v098.i16
Bessette, D. L., Mayer, L. A., Cwik, B., Vezér, M., Keller, K., Lempert, R. J., & Tuana, N. (2017). Building a values-informed mental model for New Orleans climate risk management. *Risk Analysis*, *37*(10), 1993–2004. doi: 10.1111/risa.12743
Betancourt, M. (2018, July). *A conceptual introduction to Hamiltonian Monte Carlo* (No. arXiv:1701.02434). arXiv. doi: 10.48550/arXiv.1701.02434
Bezanson, J., Karpinski, S., Shah, V. B., & Edelman, A. (2012, September). Julia: A Fast Dynamic Language for Technical Computing. *arXiv:1209.5145 [cs]*. doi: 10.48550/arXiv.1209.5145
Borgomeo, E., Mortazavi-Naeini, M., Hall, J. W., & Guillod, B. P. (2018, March). Risk, robustness and water resources planning under uncertainty. *Earth's Future*, *6*(3), 468–487. doi: 10.1002/2017ef000730
Box, G. E. P. (1976, December). Science and Statistics. *Journal of the American Statistical Association*, *71*(356), 791–799. doi: 10.1080/01621459.1976.10480949
Brown, C. M., Ghile, Y., Laverty, M., & Li, K. (2012). Decision scaling: Linking bottom-up vulnerability analysis with climate projections in the water sector. *Water Resources Research*, *48*(9). doi: 10.1029/2011wr011212
Bruneau, M., Barbato, M., Padgett, J. E., Zaghi, A. E., Mitrani-Reiser, J., & Li, Y. (2017, October). State of the art of multihazard design. *Journal of Structural Engineering*, *143*(10), 03117002. doi: 10.1061/(ASCE)ST.1943-541X.0001893
Chester, M. V., Underwood, B. S., & Samaras, C. (2020, April). Keeping infrastructure reliable under climate uncertainty. *Nature Climate Change*, 1–3. doi: 10.1038/s41558-020-0741-0
Coles, S. G., & Tawn, J. A. (1996). A Bayesian analysis of extreme rainfall data. *Journal of the Royal Statistical Society: Series C (Applied Statistics)*, *45*(4), 463–478. doi: 10.2307/2986068
de Moel, H., van Vliet, M., & Aerts, J. C. J. H. (2014, June). Evaluating the effect of flood damage-reducing measures: A case study of the unembanked area of Rotterdam, the Netherlands. *Regional Environmental Change*, *14*(3), 895–908. doi: 10.1007/s10113-013-0420-z
de Neufville, R., & Smet, K. (2019). Engineering Options Analysis (EOA). In V. A. W. J. Marchau, W. E. Walker, P. J. T. M. Bloemen, & S. W. Popper (Eds.), *Decision Making under Deep Uncertainty: From Theory to Practice* (pp. 117–132). Cham: Springer International Publishing. doi: 10.1007/978-3-030-05252-2_6
de Ruig, L. T., Haer, T., de Moel, H., Botzen, W. J. W., & Aerts, J. C. J. H. (2020, October). A micro-scale cost-benefit analysis of building-level flood risk adaptation measures in Los Angeles. *Water Resources and Economics*, *32*, 100147. doi: 10.1016/j.wre.2019.100147
DeConto, R. M., & Pollard, D. (2016, March). Contribution of Antarc-

tica to past and future sea-level rise. *Nature*, *531*(7596), 591–597. doi: 10.1038/nature17145

Doss-Gollin, J., Farnham, D. J., Ho, M., & Lall, U. (2020, April). Adaptation over fatalism: Leveraging high-impact climate disasters to boost societal resilience. *Journal of Water Resources Planning and Management*, *146*(4). doi: 10.1061/(asce)wr.1943-5452.0001190

Doss-Gollin, J., Farnham, D. J., Lall, U., & Modi, V. (2021, June). How unprecedented was the February 2021 Texas cold snap? *Environmental Research Letters*. doi: 10.1088/1748-9326/ac0278

Doss-Gollin, J., Farnham, D. J., Steinschneider, S., & Lall, U. (2019, June). Robust adaptation to multiscale climate variability. *Earth's Future*, *7*(7), 734–747. doi: 10.1029/2019ef001154

Eijgenraam, C., Kind, J., Bak, C., Brekelmans, R., den Hertog, D., Duits, M., … Kuijken, W. (2014, February). Economically efficient standards to protect the Netherlands against flooding. *INFORMS Journal on Applied Analytics*, *44*(1), 7–21. doi: 10.1287/inte.2013.0721

England, J. F., Jr., Cohn, T. A., Faber, B. A., Stedinger, J. R., Thomas, W. O., Jr., Veilleux, A. G., … Mason Jr., R. R. (2019, May). Guidelines for determining flood flow frequency Bulletin 17C. In *Techniques and methods* (Version 1.1 ed., Vol. 4-B5, p. 148). U.S.Geological Survey.

Errickson, F. C., Keller, K., Collins, W. D., Srikrishnan, V., & Anthoff, D. (2021). Equity is more important for the social cost of methane than climate uncertainty. *Nature*, *592*(7855), 564–570. doi: 10.1038/s41586-021-03386-6

Farnham, D. J., Doss-Gollin, J., & Lall, U. (2018). Regional extreme precipitation events: Robust inference from credibly simulated GCM variables. *Water Resources Research*, *54*(6). doi: 10.1002/2017wr021318

Farnham, D. J., Steinschneider, S., & Lall, U. (2017, December). Zonal wind indices to reconstruct CONUS winter precipitation. *Geophysical Research Letters*, *44*(24), 12, 236–12, 243. doi: 10.1002/2017gl075959

Fischbach, J. R., Johnson, D. R., Ortiz, D. S., Bryant, B. P., Hoover, M., & Ostwald, J. (2012, October). *Coastal Louisiana Risk Assessment Model: Technical description and 2012 Coastal Master Plan analysis results* (Technical Report No. TR-1259-CPRA). Santa Monica, CA: RAND Corporation.

Fletcher, S., Lickley, M., & Strzepek, K. (2019, April). Learning about climate change uncertainty enables flexible water infrastructure planning. *Nature Communications*, *10*(1), 1782. doi: 10.1038/s41467-019-09677-x

Fletcher, S., Strzepek, K., Alsaati, A., & de Weck, O. (2019, November). Learning and flexibility for water supply infrastructure planning under groundwater resource uncertainty. *Environmental Research Letters*, *14*(11), 114022. doi: 10.1088/1748-9326/ab4664

Fletcher, S. M., Miotti, M., Jaichander, S., Klemun, M. M., Strzepek, K., & Siddiqi, A. (2017, October). Water Supply Infrastructure Planning: Decision-Making Framework to Classify Multiple Uncertainties and Evaluate Flexible Design. *Journal of Water Resources Planning and Management*, *143*(10), 04017061. doi: 10.1061/(asce)wr.1943-5452.0000823

Garner, G. G., & Keller, K. (2018, September). Using direct policy search to identify robust strategies in adapting to uncertain sea-level rise and storm surge. *Environmental Modelling & Software*, *107*, 96–104. doi: 10.1016/j.envsoft.2018.05.006

Ge, H., Xu, K., & Ghahramani, Z. (2018, March). Turing: A Language for Flexible Probabilistic Inference. In *Proceedings of the Twenty-First International Conference on Artificial Intelligence and Statistics* (pp. 1682–1690). PMLR.

Gelman, A., & Shalizi, C. R. (2013). Philosophy and the practice of Bayesian statistics. *British Journal of Mathematical and Statistical Psychology*, *66*(1), 8–38. doi: 10.1111/j.2044-8317.2011.02037.x

Gelman, A., Vehtari, A., Simpson, D., Margossian, C. C., Carpenter, B., Yao, Y., … Modrák, M. (2020, November). Bayesian workflow. *arXiv:2011.01808 [stat]*. doi: 10.48550/arXiv.2011.01808

Groves, D. G., & Lempert, R. J. (2007, February). A new analytic method for finding policy-relevant scenarios. *Global Environmental Change*, *17*(1), 73–85. doi: 10.1016/j.gloenvcha.2006.11.006

Gupta, A., Govindaraju, R. S., Morbidelli, R., & Corradini, C. (2022). The role of prior probabilities on parameter estimation in hydrological models. *Water Resources Research*, *58*(5), e2021WR031291. doi: 10.1029/2021WR031291

Haasnoot, M., Winter, G., Brown, S., Dawson, R. J., Ward, P. J., & Eilander, D. (2021, January). Long-term sea-level rise necessitates a commitment to adaptation: A first order assessment. *Climate Risk Management*, *34*, 100355. doi: 10.1016/j.crm.2021.100355

Hausfather, Z., & Peters, G. P. (2020, January). Emissions – the 'business as usual' story is misleading. *Nature*, *577*(7792), 618–620. doi: 10.1038/d41586-020-00177-3

Helgeson, C., Keller, K., Nicholas, R. E., Srikrishnan, V., Cooper, C., Smithwick, E. A. H., & Tuana, N. (2022, May). *Integrating values to improve the relevance and inclusiveness of climate-risk research.* SocArXiv. doi: 10.31235/osf.io/c4k7d

Herman, J. D., Quinn, J. D., Steinschneider, S., Giuliani, M., & Fletcher, S. (2020, January). Climate adaptation as a control problem: Review and perspectives on dynamic water resources planning under uncertainty. *Water Resources Research*, e24389. doi: 10.1029/2019wr025502

Herman, J. D., Reed, P. M., Zeff, H. B., & Characklis, G. W. (2015, October). How should robustness be defined for water systems planning under change? *Journal of Water Resources Planning and Management*, *141*(10), 04015012. doi: 10.1061/(asce)wr.1943-5452.0000509

Ho, E., Budescu, D. V., Bosetti, V., van Vuuren, D. P., & Keller, K. (2019, August). Not all carbon dioxide emission scenarios are equally likely: A subjective expert assessment. *Climatic Change*, *155*(4), 545–561. doi: 10.1007/s10584-019-02500-y

Ho, M., Lall, U., Allaire, M., Devineni, N., Kwon, H.-H., Pal, I., … Wegner, D. (2017, February). The future role of dams in the United States of America. *Water Resources Research*, *53*(2), 982–998. doi: 10.1002/2016wr019905

Hoffman, M. D., & Gelman, A. (2011, November). The No-U-Turn Sampler: Adaptively Setting Path Lengths in Hamiltonian Monte Carlo. *arXiv:1111.4246 [stat.CO]*. doi: 10.48550/arXiv.1111.4246

Hui, R., Herman, J., Lund, J., & Madani, K. (2018, August). Adaptive water infrastructure planning for nonstationary hydrology. *Advances in Water Resources*, *118*, 83–94. doi: 10.1016/j.advwatres.2018.05.009

Huizinga, J., & Szewczyk, W. (2016). *Global flood depth-damage functions: Methodology and the database with guidelines.* LU: Publications Office of the European Union.

Johnson, D. R., Fischbach, J. R., & Ortiz, D. S. (2013, August). Estimating surge-based flood risk with the Coastal Louisiana Risk Assessment model. *Journal of Coastal Research*, *67*(sp1), 109–126. doi: 10.2112/si_67_8

Keller, K., Helgeson, C., & Srikrishnan, V. (2021). Climate risk management. *Annual Review of Earth and Planetary Sciences*, *49*(1), 95–116. doi: 10.1146/annurev-earth-080320-055847

Kopp, R. E., DeConto, R. M., Bader, D. A., Hay, C. C., Horton, R. M., Kulp, S., … Strauss, B. H. (2017). Evolving understanding of Antarctic ice-sheet physics and ambiguity in probabilistic sea-level projections. *Earth's Future*, *5*(12), 1217–1233. doi: 10.1002/2017ef000663

Kopp, R. E., Horton, R. M., Little, C. M., Mitrovica, J. X., Oppenheimer, M., Ras-

mussen, D. J., … Tebaldi, C. (2014). Probabilistic 21st and 22nd century sea-level projections at a global network of tide-gauge sites. *Earth's Future*, *2*(8), 383–406. doi: 10.1002/2014ef000239

Kousky, C., & Kunreuther, H. (2014, June). Addressing affordability in the National Flood Insurance Program. *Journal of Extreme Events*, *01*(01), 1450001. doi: 10.1142/s2345737614500018

Kreibich, H., Thieken, A. H., Petrow, T., Müller, M., & Merz, B. (2005, January). Flood loss reduction of private households due to building precautionary measures – lessons learned from the Elbe flood in August 2002. *Natural Hazards and Earth System Sciences*, *5*(1), 117–126. doi: 10.5194/nhess-5-117-2005

Lamontagne, J. R., Reed, P. M., Link, R., Calvin, K. V., Clarke, L. E., & Edmonds, J. A. (2018). Large Ensemble Analytic Framework for Consequence-Driven Discovery of Climate Change Scenarios. *Earth's Future*, *6*(3), 488–504. doi: 10.1002/2017ef000701

Lempert, R. J. (2002, May). A new decision sciences for complex systems. *Proceedings of the National Academy of Sciences*, *99*(suppl 3), 7309–7313. doi: 10.1073/pnas.082081699

Lempert, R. J., & Schlesinger, M. E. (2000, June). Robust strategies for abating climate change. *Climatic Change*, *45*(3-4), 387–401. doi: 10.1023/A:1005698407365

Lopez-Cantu, T., & Samaras, C. (2018, June). Temporal and spatial evaluation of stormwater engineering standards reveals risks and priorities across the United States. *Environmental Research Letters*, *13*(7). doi: 10.1088/1748-9326/aac696

McPhail, C., Maier, H. R., Kwakkel, J. H., Giuliani, M., Castelletti, A., & Westra, S. (2019, April). Robustness metrics: How are they calculated, when should they be used and why do they give different results? *Earth's Future*, 169–191. doi: 10.1002/2017ef000649

Merz, B., Aerts, J. C. J. H., Arnbjerg-Nielsen, K., Baldi, M., Becker, A., Bichet, A., … Nied, M. (2014). Floods and climate: Emerging perspectives for flood risk assessment and management. *Natural Hazards and Earth System Science*, *14*(7), 1921–1942. doi: 10.5194/nhess-14-1921-2014

Merz, B., Hall, J., Disse, M., & Schumann, A. (2010, March). Fluvial flood risk management in a changing world. *Natural Hazards and Earth System Sciences*, *10*(3), 509–527. doi: 10.5194/nhess-10-509-2010

Mikkola, P., Martin, O. A., Chandramouli, S., Hartmann, M., Pla, O. A., Thomas, O., … Klami, A. (2021, December). *Prior knowledge elicitation: The past, present, and future* (No. arXiv:2112.01380). arXiv. doi: 10.48550/arXiv.2112.01380

Milly, P. C. D., Betancourt, J., Falkenmark, M., Hirsch, R. M., Kundzewicz, Z. W., Lettenmaier, D. P., & Stouffer, R. J. (2008, February). Stationarity is dead: Whither water management? *Science*, *319*(5863), 573–574. doi: 10.1126/science.1151915

Moallemi, E. A., Kwakkel, J., de Haan, F. J., & Bryan, B. A. (2020, November). Exploratory modeling for analyzing coupled human-natural systems under uncertainty. *Global Environmental Change*, *65*, 102186. doi: 10.1016/j.gloenvcha.2020.102186

Moallemi, E. A., Zare, F., Reed, P. M., Elsawah, S., Ryan, M. J., & Bryan, B. A. (2020, January). Structuring and evaluating decision support processes to enhance the robustness of complex human–natural systems. *Environmental Modelling & Software*, *123*, 104551. doi: 10.1016/j.envsoft.2019.104551

Mobley, W., Atoba, K. O., & Highfield, W. E. (2020, January). Uncertainty in flood mitigation practices: Assessing the economic benefits of property acquisition and elevation in flood-prone communities. *Sustainability*, *12*(5), 2098. doi: 10.3390/su12052098

Montanari, A., & Koutsoyiannis, D. (2014, December). Modeling and mitigating natural hazards: Stationarity is immortal! *Water Resources Research*, *50*(12), 9748–9756. doi: 10.1002/2014wr016092

Moody, P., & Brown, C. (2013). Robustness indicators for evaluation under climate change: Application to the upper Great Lakes. *Water Resources Research*, *49*(6), 3576–3588. doi: 10.1002/wrcr.20228

Morgan, M. G. (1990). *Uncertainty: A guide to dealing with uncertainty in quantitative risk and policy analysis*. Cambridge [England] ;: Cambridge University Press.

Morgan, M. G. (2014, May). Use (and abuse) of expert elicitation in support of decision making for public policy. *Proceedings of the National Academy of Sciences*, *111*(20), 7176–7184. doi: 10.1073/pnas.1319946111

Moss, R. H., & Schneider, S. H. (2000). Uncertainties in the IPCC TAR: Recommendations to lead authors for more consistent assessment and reporting. In R. Pachauri, T. Taniguchi, & K. Tanaka (Eds.), *Guidance papers on the cross cutting issues of the third assessment report of the IPCC* (pp. 33–51). Geneva: World Meteorological Organization.

National Oceanographic and Atmospheric Administration. (2022). *Tides and Currents.* https://tidesandcurrents.noaa.gov/.

National Weather Service, & Office of Water Prediction. (2022, January). *Analysis of impact of nonstationary climate on NOAA Atlas 14 estimates* (Tech. Rep.).

Nofal, O. M., van de Lindt, J. W., & Do, T. Q. (2020, October). Multi-variate and single-variable flood fragility and loss approaches for buildings. *Reliability Engineering & System Safety*, *202*, 106971. doi: 10.1016/j.ress.2020.106971

Oddo, P. C., Lee, B. S., Garner, G. G., Srikrishnan, V., Reed, P. M., Forest, C. E., & Keller, K. (2017). Deep uncertainties in sea-level rise and storm surge projections: Implications for coastal flood risk management. *Risk Analysis*, *0*(0). doi: 10.1111/risa.12888

Oreskes, N., Shrader-Frechette, K., & Belitz, K. (1994, February). Verification, validation, and confirmation of numerical models in the Earth sciences. *Science*. doi: 10.1126/science.263.5147.641

Ossandón, Á., Rajagopalan, B., & Kleiber, W. (2021, September). Spatial-temporal multivariate semi-Bayesian hierarchical framework for extreme precipitation frequency analysis. *Journal of Hydrology*, *600*, 126499. doi: 10.1016/j.jhydrol.2021.126499

Perica, S., Pavlovic, S., St. Laurent, M., Trypaluk, C., Unruh, D., & Wilhite, O. (2018). *NOAA Atlas 14* (Tech. Rep. No. Volume 11 Version 2.0: Texas). Silver Spring, MD: National Weather Service, National Oceanic and Atmospheric Administration, U.S. Department of Commerce.

Perkel, J. M. (2019, July). Julia: Come for the syntax, stay for the speed. *Nature*, *572*(7767), 141–142. doi: 10.1038/d41586-019-02310-3

Piironen, J., & Vehtari, A. (2017, May). Comparison of Bayesian predictive methods for model selection. *Statistics and Computing*, *27*(3), 711–735. doi: 10.1007/s11222-016-9649-y

Poff, N. L., Brown, C. M., Grantham, T. E., Matthews, J. H., Palmer, M. A., Spence, C. M., … Baeza, A. (2015, September). Sustainable water management under future uncertainty with eco-engineering decision scaling. *Nature Climate Change*, *6*(1), 25–34. doi: 10.1038/nclimate2765

Quinn, J. D., Hadjimichael, A., Reed, P. M., & Steinschneider, S. (2020). Can exploratory modeling of water scarcity vulnerabilities and robustness be scenario neutral? *Earth's Future*, *8*(11), e2020EF001650. doi: 10.1029/2020ef001650

Quinn, J. D., Reed, P. M., Giuliani, M., & Castelletti, A. (2017). Rival framings: A framework for discovering how problem formulation uncertainties shape risk management trade-offs in water resources systems. *Water Resources Research*, *53*(8), 7208–7233. doi: 10.1002/2017wr020524

Reed, P. M., Hadjimichael, A., Malek, K., Karimi, T., Vernon, C. R., Srikrishnan, V., … Rice, J. S. (2022). *Addressing uncertainty in multisector dynamics research*. Zenodo.

Reis, J., & Shortridge, J. (2020). Impact of uncertainty parameter distribution on robust decision making outcomes for climate change adaptation under deep uncertainty. *Risk Analysis*, *40*(3), 494–511. doi: 10.1111/risa.13405

Resio, D. T. (2007, May). White paper on estimating hurricane inundation probabilities. *This Digital Resource was created from scans of the Print Resource.*.

Rözer, V., Kreibich, H., Schröter, K., Müller, M., Sairam, N., Doss-Gollin, J., … Merz, B. (2019). Probabilistic models significantly reduce uncertainty in Hurricane Harvey pluvial flood loss estimates. *Earth's Future*, *7*(4). doi: 10.1029/2018ef001074

Rözer, V., Müller, M., Bubeck, P., Kienzler, S., Thieken, A., Pech, I., … Kreibich, H. (2016, July). Coping with pluvial floods by private households. *Water*, *8*(7), 304. doi: 10.3390/w8070304

Ruckert, K. L., Srikrishnan, V., & Keller, K. (2019, August). Characterizing the deep uncertainties surrounding coastal flood hazard projections: A case study for Norfolk, VA. *Scientific Reports*, *9*(1), 1–12. doi: 10.1038/s41598-019-47587-6

Salas, J. D., Obeysekera, J., & Vogel, R. M. (2018). Techniques for assessing water infrastructure for nonstationary extreme events: A review. *Hydrological Sciences Journal*, *63*(3), 325–352. doi: 10.1080/02626667.2018.1426858

Schneider, S. H. (2001, May). What is 'dangerous' climate change? *Nature*, *411*(6833), 17–19. doi: 10.1038/35075167

Schneider, S. H. (2002, March). Can we estimate the likelihood of climatic changes at 2100? *Climatic Change*, *52*(4), 441–451. doi: http://dx.doi.org/10.1023/A:1014276210717

Seaman, J. W., Seaman, J. W., & Stamey, J. D. (2012, May). Hidden dangers of specifying noninformative priors. *The American Statistician*, *66*(2), 77–84. doi: 10.1080/00031305.2012.695938

Serinaldi, F., & Kilsby, C. G. (2015, March). Stationarity is undead: Uncertainty dominates the distribution of extremes. *Advances in Water Resources*, *77*, 17–36. doi: 10.1016/j.advwatres.2014.12.013

Sharma, S., Lee, B. S., Nicholas, R. E., & Keller, K. (2021). A safety factor approach to designing urban infrastructure for dynamic conditions. *Earth's Future*, *9*(12), e2021EF002118. doi: 10.1029/2021EF002118

Slotter, R., Trainor, J., Davidson, R., Kruse, J., & Nozick, L. (2020). Homeowner mitigation decision-making: Exploring the theory of planned behaviour approach. *Journal of Flood Risk Management*, *13*(4). doi: 10.1111/jfr3.12667

Srikrishnan, V., Guan, Y., Tol, R. S. J., & Keller, K. (2022, February). Probabilistic projections of baseline twenty-first century CO_2 emissions using a simple calibrated integrated assessment model. *Climatic Change*, *170*(3), 37. doi: 10.1007/s10584-021-03279-7

Sriver, R. L., Lempert, R. J., Wikman-Svahn, P., & Keller, K. (2018, February). Characterizing uncertain sea-level rise projections to support investment decisions. *PLOS ONE*, *13*(2), e0190641. doi: 10.1371/journal.pone.0190641

Steinschneider, S., McCrary, R., Wi, S., Mulligan, K., Mearns, L. O., & Brown, C. M. (2015, November). Expanded Decision-Scaling Framework to Select Robust Long-Term Water-System Plans under Hydroclimatic Uncertainties. *Journal of Water Resources Planning and Management*, *141*(11). doi: 10.1061/(asce)wr.1943-5452.0000536

Sweet, W., Hamlington, B., Kopp, R., Weaver, C., Barnard, P., Bekaert, D., … Dusek, G. (2022). *Global and regional sea level rise scenarios for the United States* (NOAA Technical Report No. NOS 01). Silver Spring, MD: National Oceanic and Atmospheric Administration, National Ocean Service.

Taner, M. Ü., Ray, P., & Brown, C. (2019). Incorporating multidimensional probabilistic information into robustness-based water systems planning. *Water Resources Research*, *55*(5), 3659–3679. doi: 10.1029/2018WR022909

Tarek, M., Xu, K., Trapp, M., Ge, H., & Ghahramani, Z. (2020, February). DynamicPPL: Stan-like Speed for Dynamic Probabilistic Models. *arXiv:2002.02702 [cs, stat]*. doi: 10.48550/arXiv.2002.02702

The Federal Emergency Management Agency. (2011). *Coastal construction manual* (Vol. II). Washington, D.C.: Author.

The Federal Emergency Management Agency. (2014, June). *Homeowner's guide to retrofitting: Six ways to protect your home from flooding* (Tech. Rep. No. FEMA P-312). Washington, DC: Federal Emergency Management Agency.

Toro, G. R., Resio, D. T., Divoky, D., Niedoroda, A. W., & Reed, C. (2010, January). Efficient joint-probability methods for hurricane surge frequency analysis. *Ocean Engineering*, *37*(1), 125–134. doi: 10.1016/j.oceaneng.2009.09.004

Trindade, B. C., Gold, D. F., Reed, P. M., Zeff, H. B., & Characklis, G. W. (2020, October). Water pathways: An open source stochastic simulation system for integrated water supply portfolio management and infrastructure investment planning. *Environmental Modelling & Software*, *132*, 104772. doi: 10.1016/j.envsoft.2020.104772

Trindade, B. C., Reed, P. M., & Characklis, G. W. (2019, October). Deeply uncertain pathways: Integrated multi-city regional water supply infrastructure investment and portfolio management. *Advances in Water Resources*, 103442. doi: 10.1016/j.advwatres.2019.103442

Tversky, A., & Kahneman, D. (1974, September). Judgment under uncertainty: Heuristics and biases. *Science*, *185*(4157), 1124–1131. doi: 10.1126/science.185.4157.1124

Tye, M. R., & Giovannettone. (2021). *Impacts of future weather and climate extremes on United States infrastructure*. American Society of Civil Engineers.

United States Army Corps of Engineers, Galveston District, & Texas General Land Office. (2021, August). *Coastal Texas protection and restoration feasibility study: Final feasibility report* (Tech. Rep.). Galveston, TX.

van Dantzig, D. (1956). Economic Decision Problems for Flood Prevention. *Econometrica*, *24*(3), 276–287. doi: 10.2307/1911632

van Vuuren, D. P., de Vries, B., Beusen, A., & Heuberger, P. S. C. (2008, October). Conditional probabilistic estimates of 21st century greenhouse gas emissions based on the storylines of the IPCC-SRES scenarios. *Global Environmental Change*, *18*(4), 635–654. doi: 10.1016/j.gloenvcha.2008.06.001

Vezér, M., Bakker, A., Keller, K., & Tuana, N. (2018, March). Epistemic and ethical trade-offs in decision analytical modelling. *Climatic Change*, *147*(1), 1–10. doi: 10.1007/s10584-017-2123-9

Walker, W. E., Lempert, R. J., & Kwakkel, J. H. (2013). Deep Uncertainty. In S. I. Gass & M. C. Fu (Eds.), *Encyclopedia of Operations Research and Management Science* (pp. 395–402). Boston, MA: Springer US. doi: 10.1007/978-1-4419-1153-7_1140

Wigley, T. M. L., & Raper, S. C. B. (2001, July). Interpretation of high projections for global-mean warming. *Science*, *293*(5529), 451–454. doi: 10.1126/science.1061604

Wong, T. E. (2018, December). An integration and assessment of multiple covariates of nonstationary storm surge statistical behavior by Bayesian model averaging. *Advances in Statistical Climatology, Meteorology and Oceanography*, *4*(1/2), 53–63. doi: 10.5194/ascmo-4-53-2018

Wong, T. E., Bakker, A. M. R., Ruckert, K., Applegate, P., Slangen, A. B. A., & Keller, K. (2017, July). BRICK v0.2, a simple, accessible, and transparent model framework for climate and regional sea-level projections. *Geoscientific Model Development*, *10*(7), 2741–2760. doi: 10.5194/gmd-10-2741-2017

Wong, T. E., & Keller, K. (2017). Deep uncertainty surrounding coastal flood risk projections: A case study for New Orleans. *Earth's Future*, *5*(10), 1015–1026. doi: 10.1002/2017ef000607

Xian, S., Lin, N., & Kunreuther, H. (2017, May). Optimal house elevation for reducing flood-related losses. *Journal of Hydrology*, *548*, 63–74. doi: 10.1016/j.jhydrol.2017.02.057

Zarekarizi, M., Srikrishnan, V., & Keller, K. (2020, October). Neglecting uncertainties biases house-elevation decisions to manage riverine flood risks. *Nature Communications*, *11*(1), 5361. doi: 10.1038/s41467-020-19188-9

Supporting Information for "A subjective Bayesian framework for synthesizing deep uncertainties in climate risk management"

James Doss-Gollin[1], Klaus Keller[2]

[1]Department of Civil and Environmental Engineering, Rice University

[2]Thayer School of Engineering, Dartmouth College

This document contains supplementary methods, figures, and tables for the paper "A subjective Bayesian framework for synthesizing deep uncertainties in climate risk management" by James Doss-Gollin and Klaus Keller.

S1. Supplemental methods

S1.1. Statistical distributions

To avoid ambiguity, we define here some statistical distributions used in the main text. Except where otherwise indicated, we follow the default notation of the Distributions.jl Julia package (Besançon et al., 2021).

S1.1.1. Generalized Extreme Value distribution

We parameterize the generalized extreme value (GEV) distribution as

$$f(x|\mu,\sigma,\xi) = \begin{cases} \frac{1}{\sigma}\left[1+\left(\frac{x-\mu}{\sigma}\right)\xi\right]^{-1/\xi-1}\exp\left\{-\left[1+\left(\frac{x-\mu}{\sigma}\right)\xi\right]^{-1/\xi}\right\}, & \xi \neq 0 \\ \frac{1}{\sigma}\exp\left\{-\frac{x-\mu}{\sigma}\right\}\exp\left\{-\exp\left[-\frac{x-\mu}{\sigma}\right]\right\}, & \xi = 0. \end{cases} \tag{S1}$$

Corresponding author: J. Doss-Gollin, Department of Civil and Environmental Engineering, Rice University, Houston, TX, USA (jdossgollin@rice.edu)

S1.1.2. Inverse Gamma distribution

Parameterizing the Inverse Gamma distribution as

$$f(x|\alpha,\theta) = \frac{\theta^\alpha x^{-(\alpha+1)}}{\Gamma(\alpha)} e^{-\frac{\theta}{x}}, \quad x > 0, \tag{S2}$$

the parameters α and θ can be computed from the desired mean μ and standard deviation σ as

$$\begin{aligned} \alpha &= 2 + \frac{\mu^2}{\sigma^2} \\ \theta &= \mu(\alpha - 1). \end{aligned} \tag{S3}$$

S1.1.3. Gamma distribution

We parameterize the Gamma distribution as

$$f(x|\alpha,\theta) = \frac{x^{\alpha-1} e^{-x/\theta}}{\Gamma(\alpha)\theta^\alpha}, \quad x > 0. \tag{S4}$$

S1.1.4. Plotting position

The plotting position used in fig. 5 is the Weibull ("empirical") plotting position

$$r/N+1 \tag{S5}$$

where N is the sample size and r is the order of the N observations ($r = 1$ is the largest, $r = N$ is the smallest).

S1.2. Algorithm to estimate expected damages

As discussed in section 4.3, we use a Monte Carlo integration to estimate expected damages D as a function of house elevation $h = h_0 + \delta h$ and mean relative sea level (MSL), $y(t)$. Specifically, for $m = 1, \ldots, M$:

1. draw a sample from the posterior distribution of storm surge (see eq. (3)) $\{\mu_m, \sigma_n, \xi_m\}$

2. simulate a single storm surge from this stationary GEV distribution and add the mean sea level to get total flood depth y_m^{sim}

3. calculate the flood damages for this draw by plugging the annual maximum flood depth relative to the house,$h - y'(t)$, into the deterministic HAZUS depth-damage relationship, storing this as the mth damage.

We then estimate expected annual damages as the sample mean of the M estimates.

S1.3. Surrogate model for expected annual damages

Evaluating expected annual damages for each of J simulations of sea level rise (SLR), each of N draws from the posterior distribution of storm surge, and each of T time steps for K models requires $N \times J \times T \times K$ simulations. In our model, we have $T = 70$, $N = 10\,000$, $J = 179\,232$, hence exhaustive sampling may be prohibitive.

Noticing that this function depends only on the elevation of the house relative to MSL, we develop a simple emulator for expected annual damages given this difference: $\hat{D}(h - \overline{y})$. To do this, we precompute expected annual damage for all height differences in 0.25 ft increments from -30 ft to 30 ft and fit a piecewise linear interpolation to this data. We use $K = 1 \times 10^6$ samples to fit this emulator for each of the 241 increments. This model is shown in fig. S2. Once this interpolation has been precomputed, calculating expected annual damage for a particular year only requires evaluating a piecewise linear function.

References

Besançon, M., Papamarkou, T., Anthoff, D., Arslan, A., Byrne, S., Lin, D., & Pearson, J. (2021). Distributions.jl: Definition and Modeling of Probability Distributions in the JuliaStats Ecosystem. *Journal of Statistical Software*, *98*(16). doi: 10.18637/

jss.v098.i16

Coles, S. G., & Tawn, J. A. (1996). A Bayesian analysis of extreme rainfall data. *Journal of the Royal Statistical Society: Series C (Applied Statistics)*, *45*(4), 463–478. doi: 10.2307/2986068

Gelman, A., Carlin, J. B., Stern, H. S., & Rubin, D. B. (2014). *Bayesian Data Analysis* (Third ed.). Chapman & Hall/CRC Boca Raton, FL, USA.

Gelman, A., Vehtari, A., Simpson, D., Margossian, C. C., Carpenter, B., Yao, Y., … Modrák, M. (2020, November). Bayesian workflow. *arXiv:2011.01808 [stat]*. doi: 10.48550/arXiv.2011.01808

Geyer, C. J. (1992). Practical Markov Chain Monte Carlo. *Statistical Science*, *7*(4), 473–483.

Huizinga, J., & Szewczyk, W. (2016). *Global flood depth-damage functions: Methodology and the database with guidelines*. LU: Publications Office of the European Union.

Johnson, D. R., Fischbach, J. R., & Ortiz, D. S. (2013, August). Estimating surge-based flood risk with the Coastal Louisiana Risk Assessment model. *Journal of Coastal Research*, *67*(sp1), 109–126. doi: 10.2112/si_67_8

McElreath, R. (2020). *Statistical rethinking: A Bayesian course with examples in R and Stan* (Second edition. ed.). Boca Raton ;: CRC Press, Taylor & Francis Group.

Zarekarizi, M., Srikrishnan, V., & Keller, K. (2020, October). Neglecting uncertainties biases house-elevation decisions to manage riverine flood risks. *Nature Communications*, *11*(1), 5361. doi: 10.1038/s41467-020-19188-9

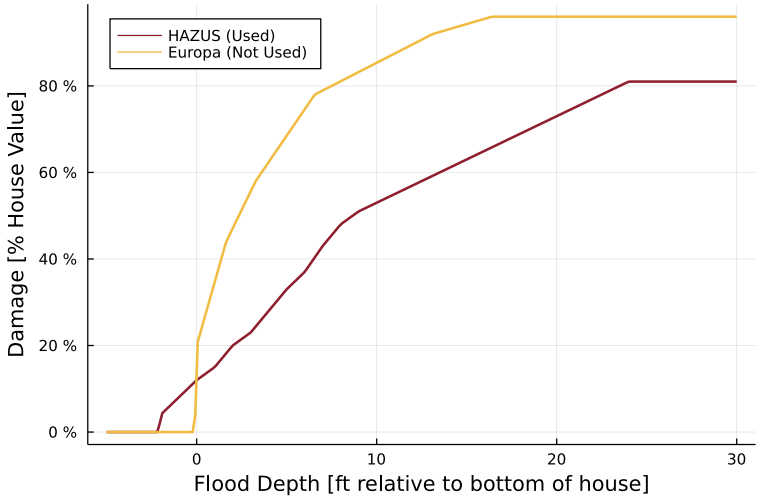

Figure S1. Depth-damage relationship. Following Zarekarizi et al. (2020), we use the HAZUS depth-damage curves. Since results are sensitive to choice of depth-damage equation, we illustrate (for comparison only) the "Europa" depth-damage relationship developed by the Joint Research Center (JRC) of the European Commission's science and knowledge service (Huizinga & Szewczyk, 2016).

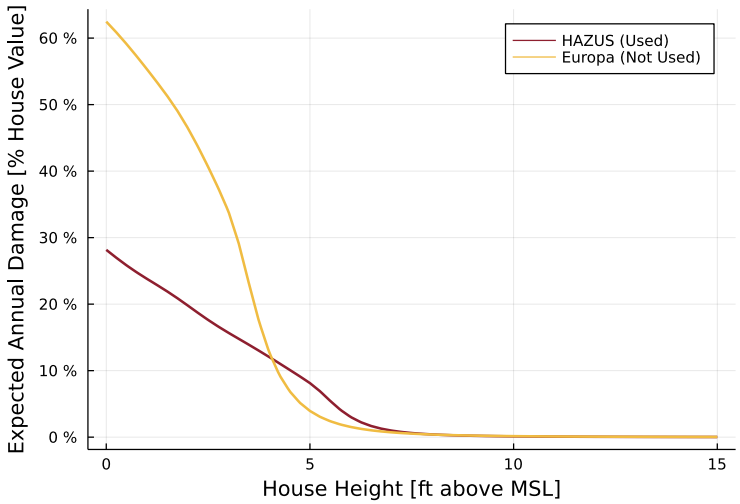

Figure S2. As discussed in section 4.3, we model expected annual damages (eq. 4) as a function of the house's elevation relative to MSL. Damages (y axis) are shown as a percentage of house value.

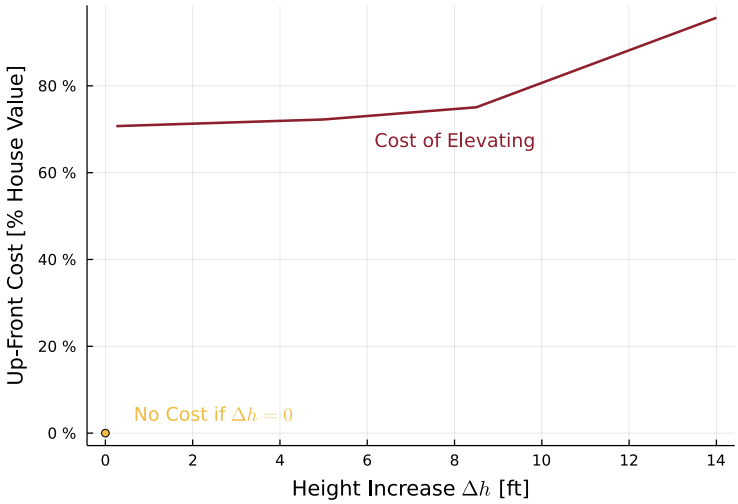

Figure S3. Following Zarekarizi et al. (2020), we model the cost of elevating a single-family house by interpolating estimates from the Coastal Louisiana Risk Assessment Model (Johnson et al., 2013). According to this model, the unit cost of elevating a house by 3-7, 7-10, and 10-14 feet is \$82.50, \$86.25, and \$103.75 per square foot, respectively, with a \$20 745 initial cost. Values are sensitive to house floor area and structural value; see table 1.

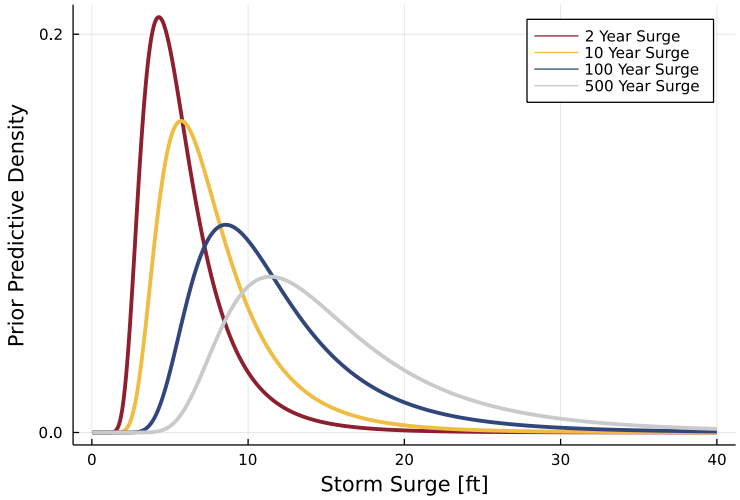

Figure S4. Prior distributions for annual maximum storm surge. Rather than apply a prior over model parameters directly, we apply a weakly informative prior over quantiles of the resulting distribution (that is, over a function of the model parameters) following Coles and Tawn (1996). See section 4.2 for details. For the 2, 10, 100, and 500 year events we apply Inverse Gamma distributions, with means 4 ft, 6 ft, 10 ft and 15 ft and standard deviations 1.5 ft, 1.75 ft, 2.25 ft and 2.75 ft, respectively.

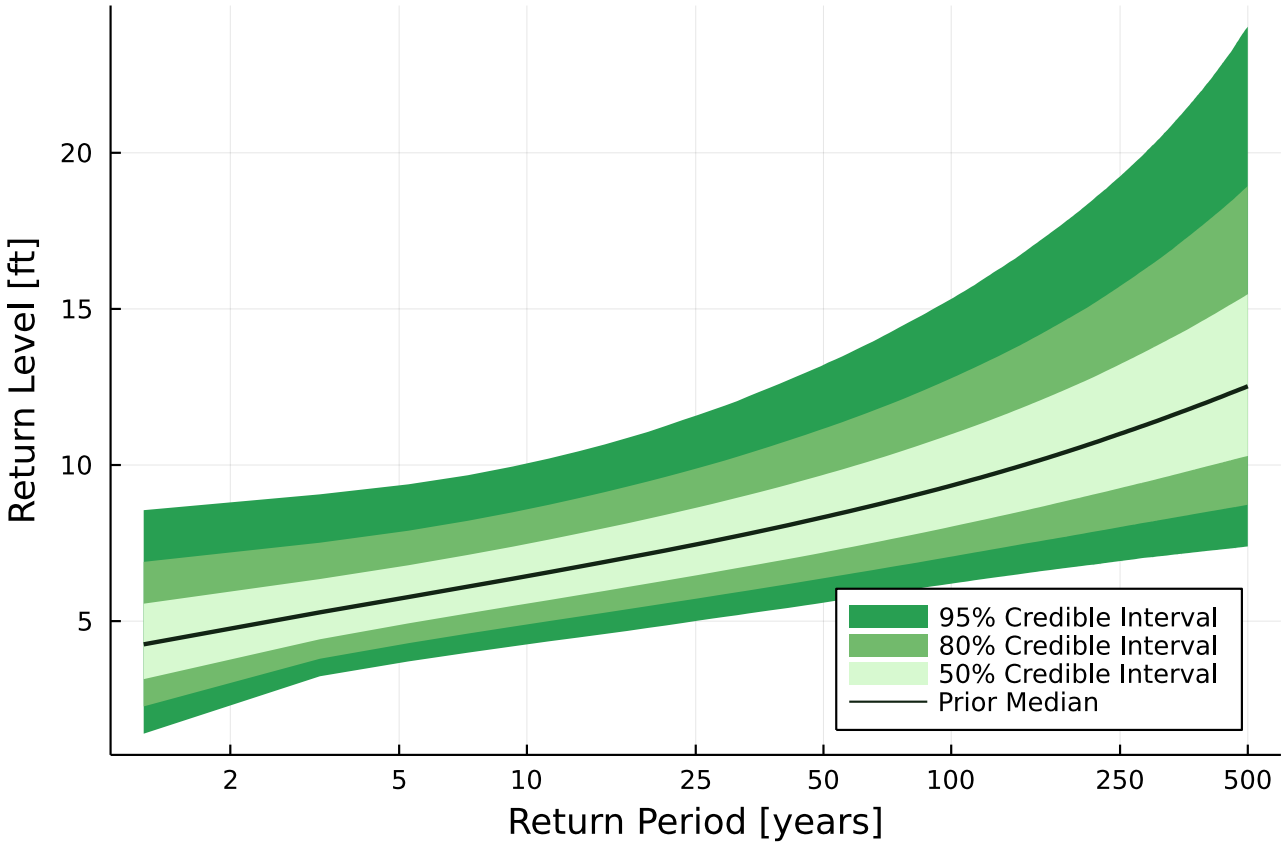

Figure S5. Implicit prior over storm surge represents large uncertainty but is consistent with basic physical reasoning (see section 4.2). The prior median (blue line) and uncertainty quantiles (shading) of the return period for different return levels of storm surge at Sewells Point, VA using prior predictive sampling (Gelman et al., 2020). This illustrates the weakly informative prior information (section 4.2) used in the analysis. These weakly informative priors were selected to be consistent with basic physical principles (*e.g.*, storm surges most years are $> 2\,\text{ft}$ but rarely exceed $20\,\text{ft}$).

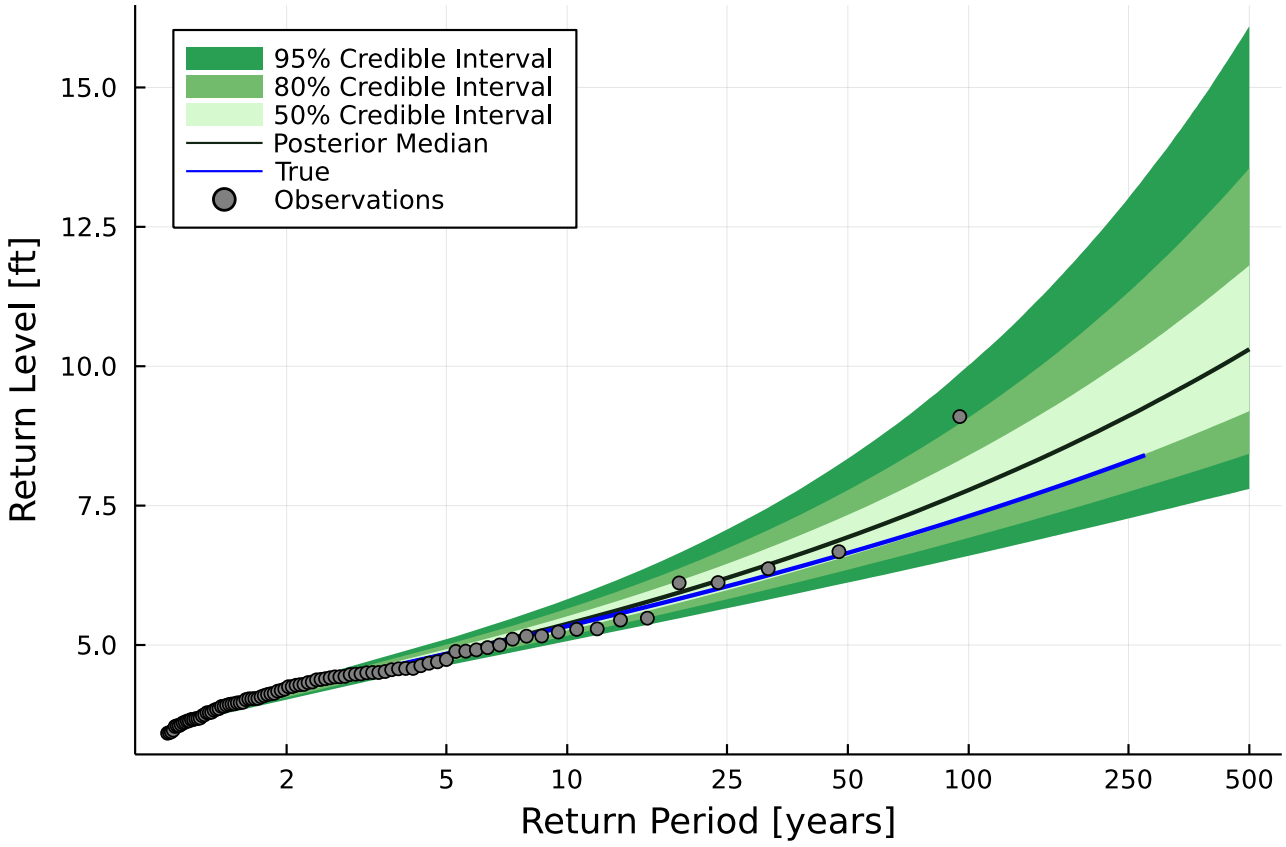

Figure S6. Synthetic data experiment as a positive control test for the GEV model of storm surge. A synthetic record (dots) was sampled from a GEV distribution with location, scale, and shape parameters of 4, 0.5, and 0.15, respectively. These samples were used to fit the Bayesian GEV model described in section 4.2; the gray shading indicates the 50, 80, and 95% posterior confidence intervals. The blue line shows the true quantiles of the (known) GEV distribution. By random chance the sample maximum has a true return period of $\gg 250$ years, which increases the upper confidence interval of the estimated return probabilities, but the true value is nevertheless within the 50% posterior confidence interval. This experiment yields similar results for alternative values of the known GEV distribution, and for different random seeds (not shown).

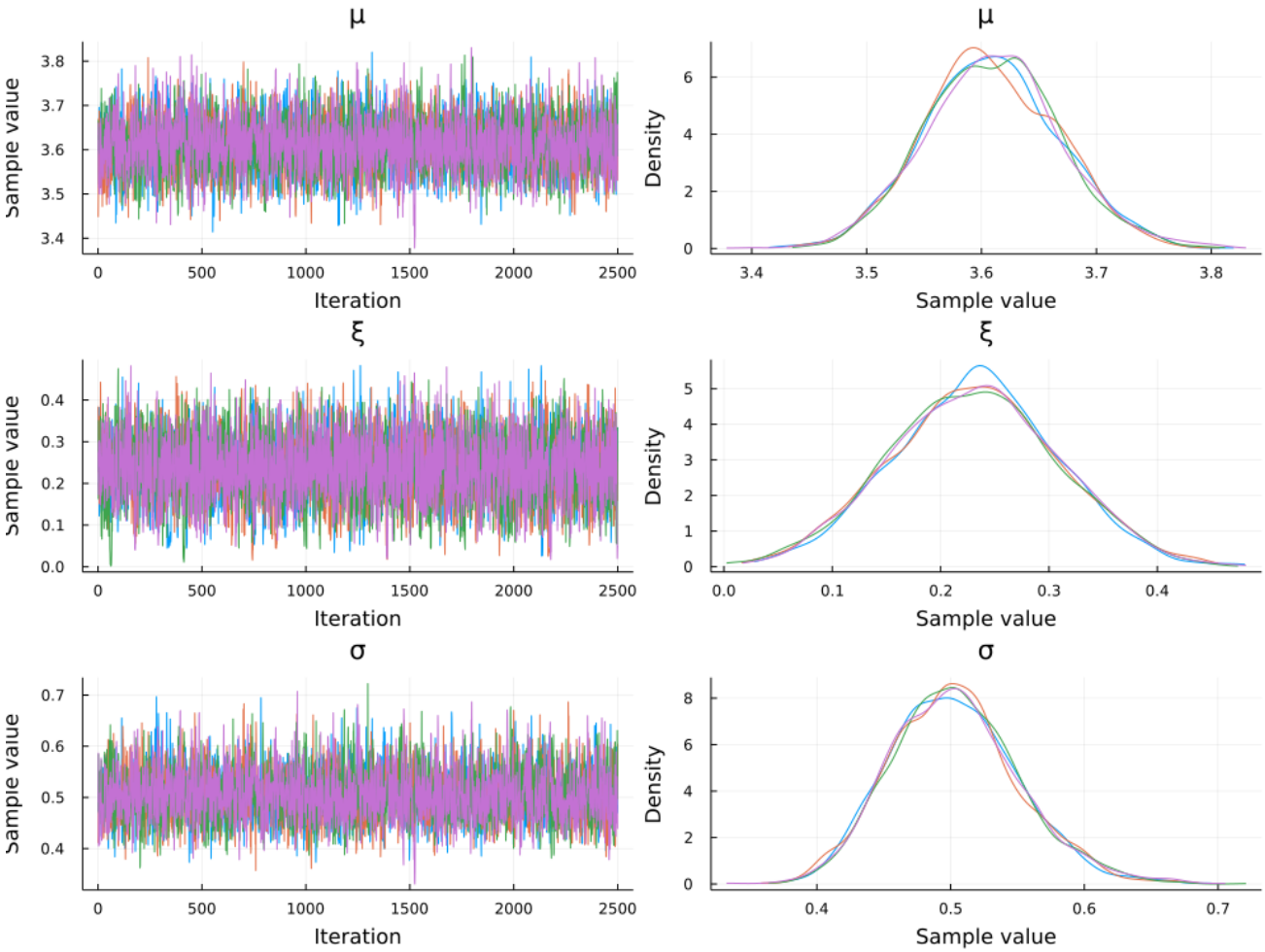

Figure S7. Markov chain diagnostic plots for posterior draws from the storm surge model. We draw 10 000 samples by running four chains of 3500 iterations each and discarding the first 1000. The mixing of the chains is consistent with, though does not guarantee, convergence.

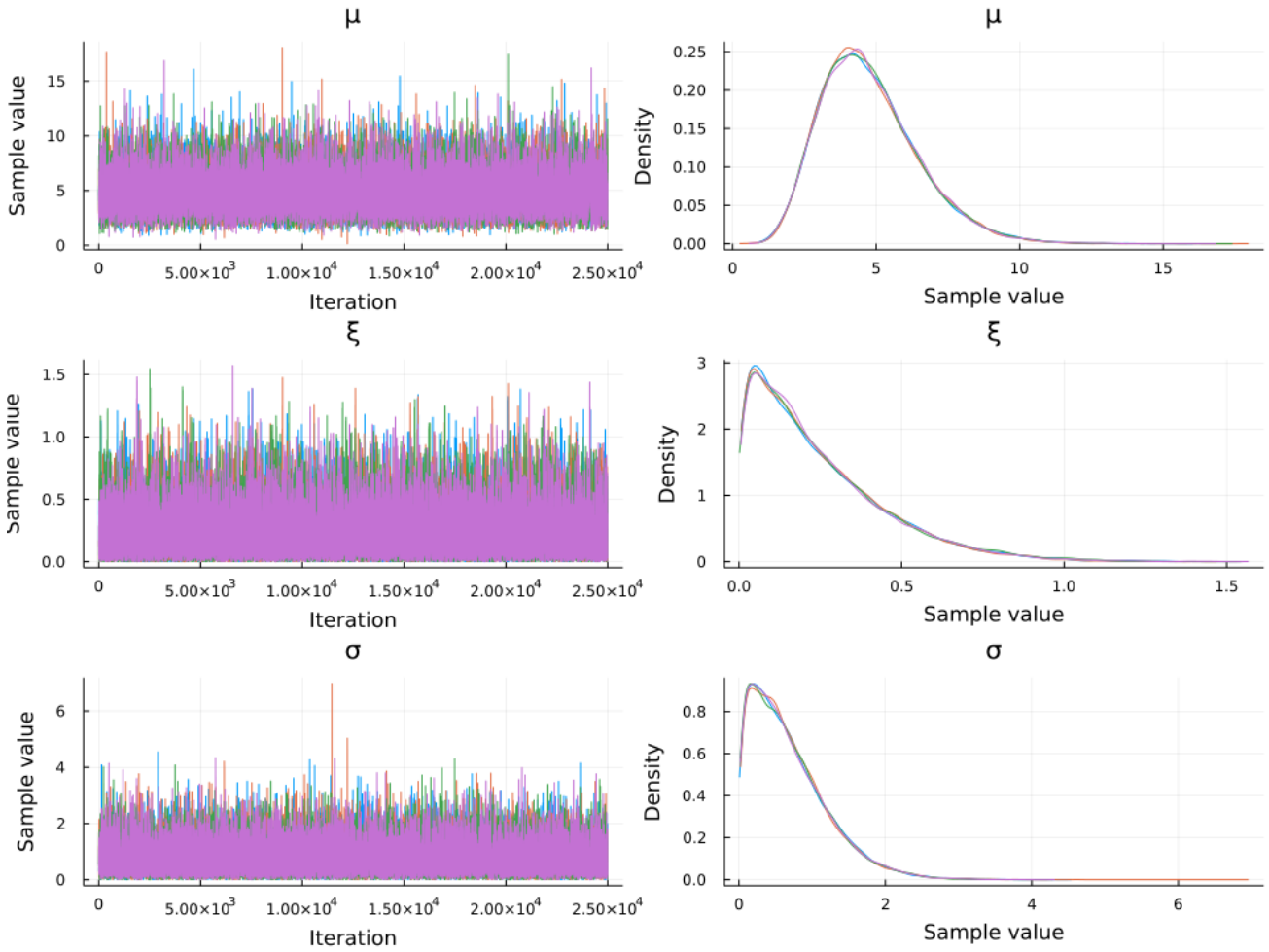

Figure S8. As fig. S7, but for draws from the prior distribution.

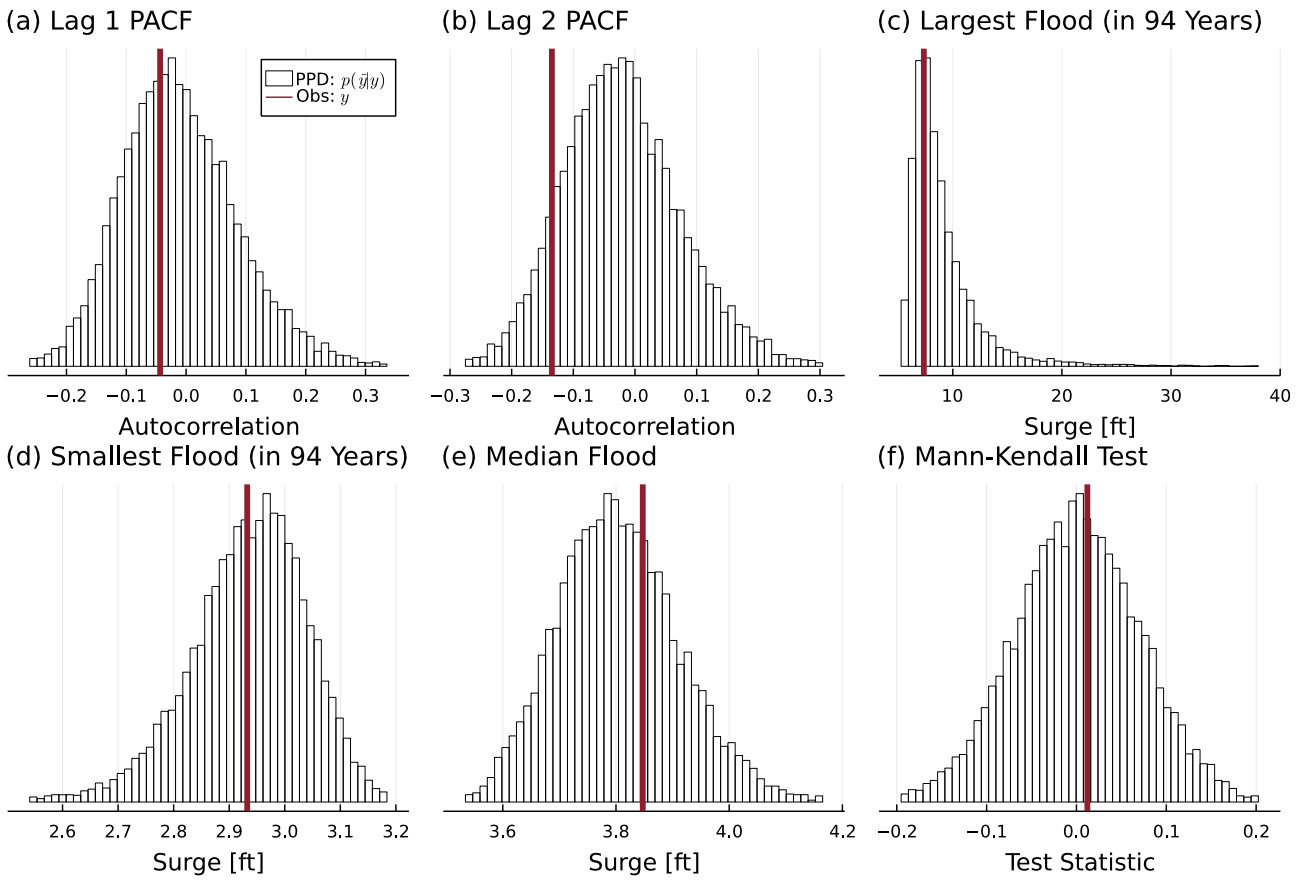

Figure S9. Posterior predictive checks for the stationary GEV storm surge model (section 4.2). Each panel shows a different test statistic: partial autocorrelation at lags 1 and 2; sample maximum; sample minimum; sample median; and Mann-Kendall trend test statistic. The histograms show the distribution of each test statistic from the posterior predictive distribution. Orange lines show the test statistic's value in the observed data. Observed values near the mode of the posterior predictive distribution are consistent with, but do not guarantee, a good fit. For further discussion of posterior predictive checks, see Chapter 6 of Gelman et al. (2014).

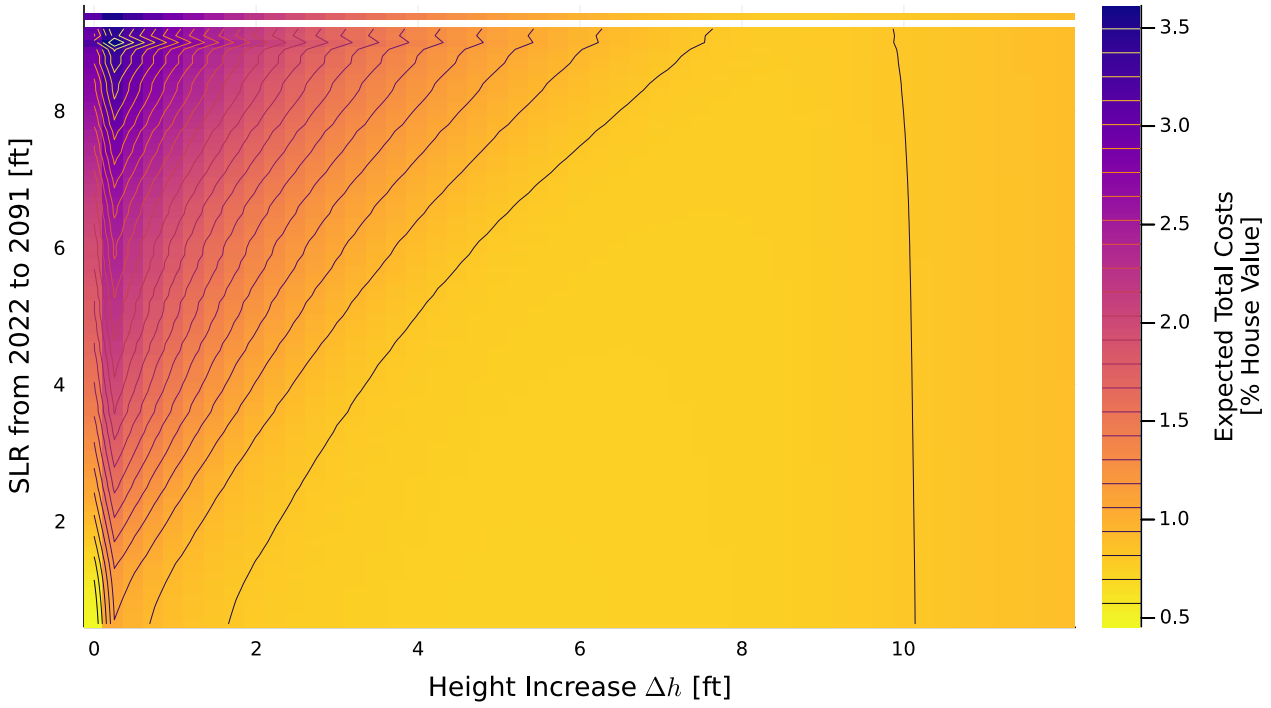

Figure S10. Expected total lifetime cost (damages plus up-front cost) as a function of SLR over the house lifetime and height increase Δh. Initial house elevation is fixed to 1 ft below the BFE. Expectations were computed for discrete values of Δh (x axis) by discretizing SOWs (y axis), then taking the sample mean over each grid cell.

Table S1. Diagnostic statistics for the Hamiltonian Monte Carlo sampling for the storm surge posterior draws. Statistics include the mean and standard deviation of each parameter, the naive standard error and Monte Carlo standard error (which measure uncertainty in the mean), the effective sample size, $\hat{R}$ diagnostic, and effective samples per second, which describes sampling speed. The naive standard error (SE) returns the standard error of the mean. The Monte Carlo standard error (MCSE) is calculated using the initial monotone sequence estimator (Geyer, 1992, pp. 473-483). The effective sample size (ESS) is a crude estimate of the number of independent samples and is calculated following Geyer (1992, pp. 473-483). The $\hat{R}$ is an indicator of the convergence of the Markov chains to the target distribution; a value $\hat{R}$ value close to one is consistent with, though does not guarantee, convergence (McElreath, 2020). For additional details see the `MCMCDiagnosticTools` package documentation.

Parameter	Mean	Stdev.	Naive SE	MCSE	ESS	$\hat{R}$
μ	3.610	0.059	0.001	0.001	4922.462	1.001
ξ	0.231	0.079	0.001	0.001	4609.415	1.001
σ	0.504	0.049	0.000	0.001	4547.881	1.001

Table S2. As table S1 but for draws from the prior distribution.

Parameter	Mean	Stdev.	Naive SE	MCSE	ESS	$\hat{R}$
μ	4.774	1.702	0.005	0.011	26657.405	1.000
ξ	0.246	0.215	0.001	0.002	11238.145	1.000
σ	0.682	0.531	0.002	0.004	24720.263	1.000